

Direct satellite observation of lightning-produced NO_x

S. Beirle¹, H. Huntrieser², and T. Wagner¹

¹Max-Planck-Institut für Chemie, Mainz, Germany

²Institut für Physik der Atmosphäre, Deutsches Zentrum für Luft- und Raumfahrt (DLR), Oberpfaffenhofen, Germany

Received: 9 July 2010 – Published in Atmos. Chem. Phys. Discuss.: 2 August 2010

Revised: 11 November 2010 – Accepted: 18 November 2010 – Published: 24 November 2010

Abstract. Lightning is an important source of NO_x in the free troposphere, especially in the tropics, with strong impact on ozone production. However, estimates of lightning NO_x (LNO_x) production efficiency (LNO_x per flash) are still quite uncertain.

In this study we present a systematic analysis of NO_2 column densities from SCIAMACHY measurements over active thunderstorms, as detected by the World-Wide Lightning Location Network (WWLLN), where the WWLLN detection efficiency was estimated using the flash climatology of the satellite lightning sensors LIS/OTD. Only events with high lightning activity are considered, where corrected WWLLN flash rate densities inside the satellite pixel within the last hour are above $1/\text{km}^2/\text{h}$. For typical SCIAMACHY ground pixels of $30 \times 60 \text{ km}^2$, this threshold corresponds to 1800 flashes over the last hour, which, for literature estimates of lightning NO_x production, should result in clearly enhanced NO_2 column densities.

From 2004–2008, we find 287 coincidences of SCIAMACHY measurements and high WWLLN flash rate densities. For some of these events, a clear enhancement of column densities of NO_2 could be observed, indeed. But overall, the measured column densities are below the expected values by more than one order of magnitude, and in most of the cases, no enhanced NO_2 could be found at all.

Our results are in contradiction to the currently accepted range of LNO_x production per flash of $15 (2\text{--}40) \times 10^{25} \text{ molec/flash}$. This probably partly results from the specific conditions for the events under investigation, i.e. events of high lightning activity in the morning (local time) and mostly (for 162 out of 287 events) over ocean.

Within the detected coincidences, the highest NO_2 column densities were observed around the US Eastcoast. This might

be partly due to interference with ground sources of NO_x being uplifted by the convective systems. However, it could also indicate that flashes in this region are particularly productive.

We conclude that current estimates of LNO_x production might be biased high for two reasons. First, we observe a high variability of NO_2 for coincident lightning events. This high variability can easily cause a publication bias, since studies reporting on high NO_x production have likely been published, while studies finding no or low amounts of NO_x might have been rejected as erroneous or not significant. Second, many estimates of LNO_x production in literature have been performed over the US, which is probably not representative for global lightning.

1 Introduction

Nitrogen oxides (NO and NO_2 , summarized as NO_x) play an important role in atmospheric chemistry by driving ozone formation and influencing the OH concentration. Lightning constitutes an important natural source of NO_x , hereafter denoted as Lightning NO_x (LNO_x). LNO_x is directly produced in the upper troposphere where background levels of NO_x are generally low and the lifetime of NO_x is of the order of a few days, i.e. several times longer than for the boundary layer (\approx hours). Hence its impact on ozone production and oxidizing capacity is quite high (e.g., Labrador et al., 2005), compared to its fraction of total NO_x production. However, estimates of the total annual NO_x release by lightning are still uncertain, and literature results differ significantly, though they seem to be converging on the range of $2\text{--}8 \text{ Tg N yr}^{-1}$ (Schumann and Huntrieser, 2007, and references therein).



Correspondence to: S. Beirle
(steffen.beirle@mpic.de)

In recent years, satellite measurements of NO₂ have become available, which have provided a valuable dataset of tropospheric NO_x with global coverage. Nadir-viewing UV-Vis satellites like GOME(1&2), SCIAMACHY, or OMI, allow the retrieval of total slant column densities (SCDs), i.e. integrated concentrations along the effective light path, of several atmospheric trace gases. For NO₂, the retrieval of tropospheric SCDs (TSCDs) requires the subtraction of the stratospheric column. Tropospheric *vertical* column densities (TVCDs), i.e. vertically integrated concentrations, are obtained by consideration of radiative transfer, involving information of ground albedo, aerosols and clouds, and the NO₂ vertical profile. Tropospheric NO₂ data from satellite has been successfully used for the investigation of NO_x sources and chemistry in many studies (see e.g. Wagner, 2008; Martin et al., 2008, and references therein).

Several studies have also investigated and quantified LNO_x using satellite NO₂ observations. Beirle et al. (2004) found a correlation of flash counts from the Lightning Imaging Sensor (LIS) with monthly mean NO₂ TSCDs from GOME over Australia, and estimated the mean LNO_x production as 2.8 (0.8–14) Tg N yr⁻¹. Boersma et al. (2005) reported on an increase of mean NO₂ TVCDs over high convective clouds, and estimated the mean LNO_x production as 1.1–6.4 Tg N yr⁻¹ from correlations of NO₂ TVCDs with parameterized flash rates. Martin et al. (2007) constrain the mean annual LNO_x production to 6 (4–8) Tg N by comparing satellite observations of NO₂, O₃ and HNO₃ to a global chemical transport model. (Even the chemistry of the middle atmosphere is affected by lightning as has been shown by Arnone et al. (2008) who report on enhancements of NO₂ from MIPAS of about 10% around the stratopause due to sprites.)

These approaches consider mean NO₂ column densities for time periods of months to years. As lightning activity over continents peaks in the late afternoon, whereas current UV/vis satellite instruments measure NO₂ in the morning (GOME, GOME2, SCIAMACHY) or shortly after noon (OMI), the potentially present LNO_x is – to large part – aged. Consequently, spatial patterns of the LNO_x produced by individual thunderstorms are lost, and the averaged NO₂ enhancements are smeared out, and generally low. Thus, the impact of systematic errors within the retrieval is quite high. Especially uncertainties of the estimation of stratospheric column densities of the order of 0.5×10^{15} molec/cm² (Boersma et al., 2004) can strongly bias spatial averages over clean regions. Also spectral interferences of ground absorption features with the NO₂ cross-section can lead to biased SCDs of the same order of magnitude (Beirle et al., 2010). Finally, to estimate the NO_x production from mean NO₂ VCDs, information on the NO_x *lifetime* is required (or a chemical model has to be involved), which is also uncertain and, as a further complication, strongly height dependent. These difficulties can be overcome by investigating *direct* observations of freshly pro-

duced LNO_x over active thunderstorm: Beirle et al. (2006) analyzed a mesoscale convective system in the Gulf of Mexico in August 2000, which coincides with the GOME overpass in space and time. Individual GOME TSCDs are up to 10×10^{15} molec/cm². By roughly estimating the satellite's sensitivity for NO₂ in cumulonimbus clouds, and relating the observed NO₂ TSCDs to flashes detected by the US National Lightning Detection Network NLDN, a mean LNO_x production of 90 (32–240) mol/flash, corresponding to $5.4 (1.9–14.5) \times 10^{25}$ molec/flash, was derived. Note that for this estimate it was assumed that the enhanced NO₂ TSCD is completely due to lightning. In case of contributions of anthropogenic outflow from the US, the estimated LNO_x production would be even lower. Bucselá et al. (2010) analyzed OMI NO₂ TVCDs within the TC4 campaign around Costa Rica and report on four days with lightning-related enhancements of OMI NO₂ TVCDs. Involving in-situ NO₂ profile measurements from the DC-8 aircraft missions, and flash counts from lightning networks, they estimate LNO_x production per flash in the range of $\approx 100–250$ mol/flash, which corresponds to $6–15 \times 10^{25}$ molec/flash.

For such direct observations, which generally imply satellite measurements under cloudy conditions, the aspect of the sensitivity is particularly important for quantitative analyses. The sensitivity of satellite observations can be expressed by the air mass factor (AMF) defined as the ratio of slant- to vertical column densities. Hild et al. (2002) analyzed AMFs for NO₂ for cumulonimbus clouds, and found high sensitivity for NO₂ at the cloud top, decreasing (approximately linear) to almost zero at the cloud bottom. Beirle et al. (2009) calculated NO₂ AMFs for an ensemble of lightning scenarios from a cloud-resolving model, and in particular established a link between the measured NO₂ TSCD to the actual NO_x TVCD by considering the height-dependent NO_x partitioning. Since the NO₂/NO_x ratio decreases with altitude due to decreasing temperatures and increasing actinic flux, the sensitivity for NO_x, in contrast to the box-AMFs for NO₂, is not highest at the cloud top, but instead in the middle of the cloud. As result from Beirle et al. (2009), an overall quite high sensitivity of satellite observations for LNO_x was determined. This leads to the straightforward expectation that events of high lightning activity, which will be defined quantitatively in Sect. 2.4, should produce an amount of LNO_x that would result in enhanced NO₂ TSCDs clearly detectable from space.

In this study, we make use of the global dataset of SCIAMACHY NO₂ TSCDs, combined with global lightning data provided by WWLLN, to systematically search for events of high lightning activity and check our current understanding of LNO_x production. In addition, the global perspective – though limited by the low detection efficiency of WWLLN in some regions, and the restriction of SCIAMACHY to morning time – in principle allows to investigate possible systematic differences in regional LNO_x productivity.

Table 1. List of acronyms and symbols used in this study.

Symbol	Acronym	Explanation
	LIS	Lightning imaging sensor
	OTD	Optical transient detector
	SCIAMACHY	Scanning Imaging Absorption spectroMeter for Atmospheric CHartographY
	TMI	TRMM microwave imager
	TRMM	Tropical rainfall measuring mission
	WLLN	World Wide Lightning Location Network
	CG	Cloud-to-ground flash
	IC	Intra-cloud
	PCT	Polarization-corrected temperature
<i>S</i>	TSCD	Tropospheric slant column density
<i>V</i>	TVCD	Tropospheric vertical column density
	AMF	Air Mass Factor
<i>E</i>		Sensitivity (see Eq. 1)
<i>F</i>	FRD	Flash rate density
<i>D</i>	DE	Detection efficiency
<i>P</i>	PE	Production efficiency (LNO _x per flash)

2 Data and methods

We perform a systematic analysis of NO₂ column densities during and shortly after events of high lightning activity. NO₂ data is derived from the SCIAMACHY instrument (Sect. 2.1), where the specific viewing conditions during thunderstorms and their impact on the sensitivity of satellite measurements is taken into account (Sect. 2.2). Lightning information is taken from the World-Wide Lightning Location Network (WLLN, Sect. 2.3), which provides global and continuous lightning information. For quantitative interpretation of the WLLN flash counts, the WLLN detection efficiency (DE) is estimated using the flash climatology derived from LIS/OTD satellite measurements. In Sect. 2.4, the definition for “high” lightning activity is given. Finally, in Sect. 2.5, the observed NO₂ TSCDs are set in relation to the number of WLLN flashes, and the LNO_x production efficiency is derived for each event.

To assist the reader, Table 1 gives an overview of the acronyms and symbols used in this study.

2.1 SCIAMACHY NO₂ column densities

The Scanning Imaging Absorption spectroMeter for Atmospheric CHartographY, SCIAMACHY (Bovensmann et al., 1999), was launched onboard the ESA satellite ENVISAT in March 2002. ENVISAT orbits the Earth in a sun-synchronous orbit with a local equator crossing time of about 10:00 a.m. in descending node.

SCIAMACHY measures Earthshine spectra from the UV to the NIR with a spectral resolution of 0.22–1.48 nm. In nadir geometry, the instrument performs an across-track scan of about ±32°, equivalent to a swath-width of

960 km. The footprint of a single nadir observation is typically 30 × 60 km². Global cover of nadir measurements is achieved after 6 days.

Total SCDs of NO₂ are derived from SCIAMACHY nadir spectra using Differential Optical Absorption Spectroscopy DOAS (Platt and Stutz, 2008). Cross-sections of O₃, NO₂ (at 220 K), O₄, H₂O and CHOCHO are fitted in the spectral range 430.8–459.5 nm. In addition, Ring spectra, accounting for inelastic scattering in the atmosphere (rotational Raman) as well as in liquid water (vibrational Raman), an absorption cross-section of liquid water, and a polynomial of degree 5 are included in the fit procedure. A daily solar measurement is used as Fraunhofer reference spectrum. The fit error of NO₂ SCDs is below 0.5 × 10¹⁵ molec/cm².

The stratospheric fraction of total SCDs as function of latitude is estimated in a reference sector over the remote Pacific. Longitudinal variations of the stratospheric field, which occur especially in cases of asymmetric polar vortices, are corrected using SCIAMACHY limb observations as described in Beirle et al. (2010). After subtracting the estimated stratospheric field from total SCDs, tropospheric SCDs (TSCDs) of NO₂ are derived. The uncertainty of the stratospheric estimation (in terms of SCDs) is of the order of typically 0.5 to 1 × 10¹⁵ molec/cm² for low and midlatitudes (see Fig. 6c in Beirle et al., 2010).

2.2 Sensitivity of satellite observations for freshly produced LNO_x

For a quantitative interpretation of NO₂ TSCDs for lightning conditions, the extreme viewing conditions under cumulonimbus clouds have to be considered. For this purpose, Beirle et al. (2009) determined the “sensitivity” *E*, defined as ratio of NO₂ TSCD (i.e. the NO₂ SCD observed from space after stratospheric correction) and the TVCD of NO_x (i.e. the vertically integrated NO_x column, which directly results from the totally released LNO_x):

$$E := S_{\text{NO}_2} / V_{\text{NO}_x}. \quad (1)$$

This is a modification of the “classical” AMF description, which is necessary to account for the height-dependencies of *both*, the NO₂ sensitivity (or box-AMF) and the NO₂/NO_x partitioning *simultaneously*. In Beirle et al. (2009), values for *S*_{NO₂}, and thus *E*, were calculated using profiles of NO₂, NO_x, and hydrometeors from a cloud-resolving chemistry model for a simulation of a one week thunderstorm episode in the TOGA COARE/CEPEX region, combined with a radiative transfer model.

The NO₂/NO_x ratio at the ground is about 0.7 (cloud free) up to 1 (clouded). It decreases approximately linearly with altitude down to values below 0.1 in the upper troposphere due to the high actinic flux and the low temperatures. Box-AMFs for NO₂ are almost zero below a cloud, and reach values of more than 4 at the top of a cb cloud due to multiple scattering (compare Hild et al., 2002).

As a consequence of these opposite height dependencies of the NO₂/NO_x ratio and the NO₂ box-AMF, the sensitivity E of satellite observations for LNO_x is

- Low (<0.1) at the cloud top and above: box-AMFs for NO₂ are high, indeed, but there is almost no NO₂ to be seen due to the low [NO₂]/[NO_x] ratio <0.1 .
- Maximum (≈ 1) in the cloud middle: here, NO₂ box-AMFs are still high (≈ 2), and there is enough NO_x present in form of NO₂ to be detected from space.
- Decreasing towards the cloud bottom, due to the decrease in NO₂ box-AMFs.
- Almost zero below the cloud due to the cloud shielding.

For the simulated LNO_x profiles, Beirle et al. (2009) find a mean sensitivity E of 0.46 with a standard deviation of 0.09. I.e., for a true LNO_x TVCD of 1×10^{15} molec/cm², it is expected to observe a NO₂ TSCD of 0.46×10^{15} molec/cm² from satellite. Remarkably, the values for E are almost independent on cloud optical thickness, i.e. they are valid for the core, the anvil, and the outflow of a thunderstorm likewise. This is a consequence of the effects of clouds on both, the [NO₂]/[NO_x] ratio and the NO₂ box-AMF, combined with the different mean NO_x profiles for core (almost homogeneous) and outflow (C-shape), within the model study.

In the following, we apply this estimate of $E = 0.46$ for the transformation of measured NO₂ TSCDs into NO_x TVCDs.

2.3 The WWLLN

For the identification of satellite measurements of NO₂ coinciding with (or shortly after) events of high lightning activity, *continuous* lightning data is required. This is provided by the ground-based WWLLN.

WWLLN started operation as global lightning location network in 2003 (Dowden et al., 2008). It consists of ≈ 20 – 30 sensors around the world detecting “sferics” caused by lightning in the very low frequency (VLF) band (6 to 22 kHz). A lightning stroke is identified if a sferic is detected by at least 5 WWLLN stations, and localized using the time of group arrival (Dowden et al., 2002).

The detection efficiency (DE) of WWLLN depends e.g. on the flash type (cloud-to-ground vs. intra-cloud): WWLLN is primarily focussing on the detection of cloud-to-ground (CG) flashes with well-defined return stroke peak currents (Rodger et al., 2006). However, Jacobson et al., 2006, showed that WWLLN is also capable of detecting intra-cloud (IC) flashes with similar DE, as long as their peak current is sufficiently high.

WWLLN only detects strokes with peak currents above ≈ 10 kA, with increasing DE for peak currents up to 50 kA. Above this level, the DE is not increasing further (Jacobson et al., 2006; Rodger et al., 2006, 2009).

In addition, the DE varies regionally and temporally, depending on the number and spatial distribution of participating ground stations. Note that the DE increased from 2007 on by about 63% (relative) due to an algorithm upgrade (Rodger et al., 2009). This algorithm update was meanwhile also used to reprocess the complete WWLLN timeseries, but in this study, the older version was used.

In order to quantify the actual number of flashes, we estimate the WWLLN DE as function of time and place. For this purpose, calibrated global lightning information is needed, which is provided by the flash climatology from combined LIS/OTD measurements (LIS: Lightning Imaging Sensor; OTD: Optical Transient Detector). We thus relate annual mean WWLLN flash rate densities (FRD) $F_{\text{WWLLN}}^{\text{annual}}$, i.e. flashes per area and year, to the corresponding climatological LIS/OTD flash rate densities $F_{\text{LIS/OTD}}$. For each year, we define this ratio as “climatological” WWLLN DE D_{clim} , given as function of place.

$$D_{\text{clim}} := \frac{F_{\text{WWLLN}}^{\text{annual}}}{F_{\text{LIS/OTD}}}. \quad (2)$$

Note that we thereby (a) assume that the LIS/OTD climatology is “true” and (b) implicitly also correct for probable dependencies of WWLLN DE on flash type, since LIS and OTD are sensitive for CG and IC flashes likewise.

Regions with low LIS/OTD FRD (< 1 /km²/year) are skipped (i.e., D_{clim} is not defined) to avoid small denominators.

For the quantification of flashes within the satellite pixel (see Sects. 2.4 and 2.5), we define a corrected WWLLN FRD $F_{\text{WWLLN}}^{\text{corr}}$ as

$$F_{\text{WWLLN}}^{\text{corr}} := F_{\text{WWLLN}} / D_{\text{clim}}. \quad (3)$$

To limit the upscaling of very low FRD, we only consider regions with $D_{\text{clim}} > 1\%$ in the following.

A detailed description of our procedure to estimate annual WWLLN DE, including maps of the resulting DEs, comparisons to literature estimates of DE, a discussion on the diurnal cycle, and comparisons of individual WWLLN and LIS counts for selected individual events, are presented in Appendix A.

2.4 Definition of “high” lightning activity

In this study, we focus on SCIAMACHY NO₂ measurements coinciding in time and space with high lightning activity, also simply denoted as “events” hereafter. The WWLLN flash counts within each satellite groundpixel are summed up over the last 60 min prior to the SCIAMACHY measurement. A coincidence is considered to be an “event” if the respective flash rate density $F_{\text{WWLLN}}^{\text{corr}}$, i.e. the sum of measured WWLLN flashes within the satellite pixel over the last 60 min, scaled by $1/D_{\text{clim}}$, is above 1 /km²/h. For a typical SCIAMACHY ground pixel of 30×60 km², this FRD corresponds to 1800 flashes within the last hour.

Note that only flashes of the previous 60 min are counted; older flashes are not considered. Thus, the derived FRD is rather a *lower bound* for the actual number of flashes.

Events close to anthropogenic sources of NO_x are potentially affected by ground NO_x sources being uplifted by convective systems. Therefore, we define a “pollution mask” from the mean global distribution of NO₂ TSCDs (i.e., regions where the annual mean SCIAMACHY TSCD is above 3×10^{15} molec/cm², plus a band of 500 km around, which basically masks polluted regions in continental and coastal US, Europe, and China) to limit the interference of anthropogenic NO_x. However, the latter may still occasionally occur outside the pollution mask in case of transport in the upper troposphere, and also NO_x from biomass burning or soil emissions might interfere with LNO_x.

By our rigid definition of high lightning activity, however, we particularly focus on *fresh* LNO_x, where we can expect a direct spatial correlation of flash occurrence and the NO₂ signal.

2.5 Relation of NO₂ TSCD and WWLLN FRD

Our goal is the clear identification of fresh lightning NO_x in the NO₂ TSCD of individual SCIAMACHY ground pixels, i.e. a well defined spatial and temporal match. The dimensions of a SCIAMACHY ground pixel are 30×60 km². This dimension corresponds approximately to a time interval of 1 h, as wind speeds in the upper troposphere are of the order of 10–20 m/s (compare Huntrieser et al., 2008, Table 4c therein). We thus consider flashes for 1 h back in time.

For the detected events, we relate the observed NO₂ TSCDs to the respective WWLLN FRD. We therefore assume that NO_x contributions from sources other than lightning are negligible, and that the loss of LNO_x due to chemical transformations or outflow/dilution can be neglected within the considered time period of $\Delta T = 1$ h and for the area of a SCIAMACHY ground pixel of 30×60 km².

The NO_x TVCD V_{NO_x} due to lightning, i.e. the vertically integrated LNO_x concentration, is then given as

$$V_{\text{NO}_x} = F \times \Delta T \times P, \quad (4)$$

with F being the flash rate density (flashes per time per area), i.e. $F \times \Delta T$ being a flash density (flashes per area), and P the LNO_x production per flash, denoted as “Production Efficiency” (PE) below. In the review of Schumann and Huntrieser (2007), the best estimate for P is given as $15(2\text{--}40) \times 10^{25}$ molec [NO_x]/flash (Table 21 therein; note that this estimate is based on several studies with different methodologies, and that for the contributing field measurements, different lightning detecting systems have been used). For our threshold FRD of 1 /km²/h and the considered time period ΔT of 1 h, we thus expect a LNO_x TVCD of 15×10^{15} molec/cm². This corresponds to a NO₂ TSCD of 6.9×10^{15} molec/cm² (Eq. 1 with $E = 0.46$). Such high

NO₂ TSCDs are far above the DOAS fit noise, the uncertainty of the stratospheric estimation, or the NO₂ background TSCDs for the considered “unpolluted” regions (typically about $0\text{--}1 \times 10^{15}$ molec/cm²), and would be clearly visible from space.

For each event, an individual PE P_{event} can be estimated from the measured NO₂ SCD and the derived WWLLN FRD, using Eqs. (4), (1) and (3):

$$P_{\text{event}} = \frac{V_{\text{NO}_x}}{F_{\text{event}} \times \Delta T} = \frac{S_{\text{NO}_2}/E}{F_{\text{WWLLN}}^{\text{corr}} \times \Delta T}. \quad (5)$$

Note that, by this definition, P_{event} is *overestimated* whenever lightning activity more than 1 h ago can not be neglected.

3 Results

A systematic search of NO₂ column measurements from SCIAMACHY for coincident lightning results in 287 events (as defined in Sect. 2.4) for the period 2004–2008. As expected, during (or shortly after) active thunderstorms, all satellite pixels for the detected events are cloud covered, with a mean FRESCO cloud fraction of 0.97 and a mean cloud height of 10.6 km (note that FRESCO cloud heights approximately correspond to the cloud *middle* (Wang et al., 2008), and all events are thus deep convective cases reaching the upper troposphere). Figure 1 shows the global distribution of the detected events. In addition, the derived Production Efficiency P_{event} (Eq. 5) is color-coded. Some selected events, which are discussed in detail below, are labelled by their event-ID (see also Table 2).

The spatial distribution of the detected events (which is different from the general global distribution of lightning, compare Fig. A1 in Appendix A) is affected by D_{clim} , the pollution mask, and morning-time flash characteristics. Most events are found around the Carribean Sea and in Indonesia/Australia, where WWLLDN DE is quite high (about 5% up to 20%), whereas only few events have been found in Central Africa, as a consequence of the DE threshold of 1%. The pollution mask removes some events in the continental South-Eastern US, Southern Europe, and South-East Asia. As the diurnal cycle of continental lightning activity has a distinct minimum around 10:00 a.m. LT, while it is rather flat over oceans (compare Fig. A4 in Appendix A), many events (162) have been found over ocean.

Events with relative high PE (red dots in Fig. 1) agglomerate east from Florida and in the northern Gulf of Mexico, where already a clear coincidence of lightning and strongly enhanced NO₂ TSCDs has been reported (Beirle et al., 2006). In contrast, in the northwest of Australia, where many events occurred, values for P_{event} are rather low (blue).

Figure 2 shows a scatterplot of NO₂ TSCDs versus FRD for the detected events. The black line indicates the linear relation of Eq. (4) with a mean PE of

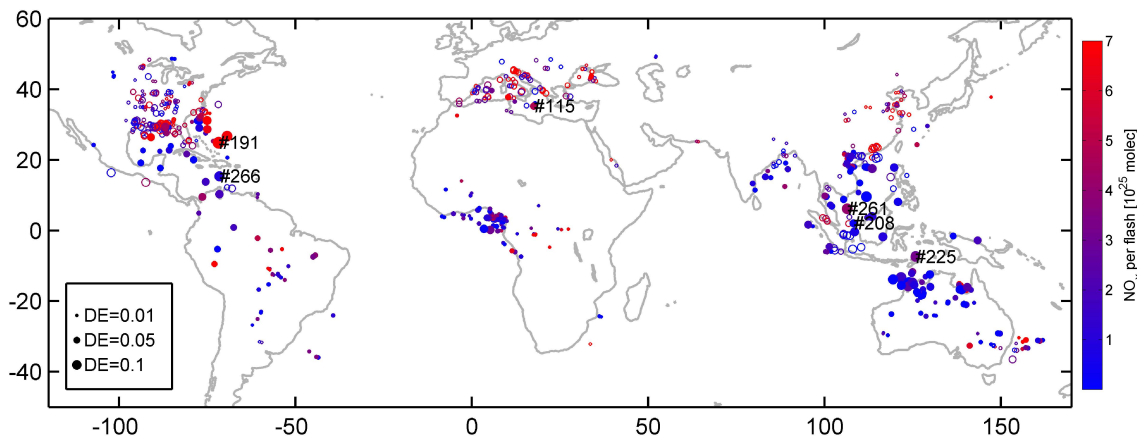


Fig. 1. Global map of events of high lightning activity coinciding with SCIAMACHY overpasses. The colors indicate the production efficiency, i.e. the LNO_x production per flash P_{event} , for the assumptions made (see Sect. 2.4). The size of the circles indicates the estimated WWLLN DE D_{clim} . Open circles indicate probably “polluted” events as defined by a pollution mask (see text). Some selected events, which are discussed in detail below, are labelled by their event ID.

Table 2. Selected events of high lightning activity (compare Figs. 3–5 and Sect. 2.4).

Category	Event ID	Date	FRD [$\frac{1}{\text{km}^2\text{h}}$]	NO ₂ TSCD [$10^{15} \frac{\text{molec}}{\text{cm}^2}$]	Spatial Corr. (R) ¹	PE [$10^{25} \frac{\text{molec}}{\text{flash}}$]	WWLLN DE [%]	Latitude [°]	Longitude [°]	Cloud fraction ²	Cloud height ² [km]
A	#115	16 Oct 2006	2.9	4.6	0.04	3.5	5.5	35.3	17.5	1.0	10.9
A	#191	12 May 2007	1.0	5.8	0.25	12.3	15.7	24.9	−71.9	1.0	10.4
C	#208	20 Aug 2007	5.8	0.5	−0.03	0.2	7.2	2.1	108.2	1.0	12.1
B	#225	22 Nov 2007	2.2	2.4	0.52	2.3	10.7	−7.4	125.7	1.0	12.6
B	#261	13 May 2008	1.7	2.3	0.47	2.9	12.7	6.2	106.4	1.0	12.7
C	#266	15 Jul 2008	1.0	0.3	−0.06	0.7	11.3	15.4	−71.6	1.0	11.2

¹ The “spatial correlation” is defined as correlation coefficient R between NO₂ TSCDs and FRDs for the ground pixels within $\pm 2^\circ$ latitude and $\pm 3^\circ$ longitude of the respective event.

² From FRESCO+ (Wang et al., 2008).

$P=15 \times 10^{25}$ molec/flash and a sensitivity E of 0.46. From Fig. 2, we can conclude the following basic results of our systematic search for LNO_x for events of high lightning activity:

1. The observed NO₂ TSCDs are generally far below the expected range of about $5\text{--}10 \times 10^{15}$ molec/cm² for a FRD of about 1, and the derived PE is far lower than values given in literature for most events.
2. In contrast to our expectations, the events’ NO₂ TSCDs are not correlated to WWLLN flash rate densities ($R=0.04$). Therefore, we abandon to give an estimate of a “mean” PE in this study, which would be proportional to the slope of a – meaningless – linear fit to the data points in Fig. 2.
3. In *some* cases, a clear (spatial) coincidence of enhanced NO₂ due to lightning could be found, similar to the case study of enhanced NO₂ TSCDs observed from GOME in the Gulf of Mexico in August 2000 reported in Beirle et al., 2006. But for many events of high lightning ac-

tivity, *no* enhanced NO₂ could be observed at all. We find 136 events with $P_{\text{event}} < 1 \times 10^{25}$ molec/flash.

Below we discuss some representative events, covering the range of observed PEs, in detail, and show spatial patterns of WWLLN flashes and NO₂ TSCDs. We focus on events with high WWLLN detection efficiencies, to limit upscaling of WWLLN FRD with respective uncertainties. Consequently, most examples are taken after 2007, when WWLLN DE increased due to an improved algorithm (Rodger et al., 2009). Nevertheless, the general findings do not depend on D_{clim} , and events for lower DE are similarly variable.

We show illustrative examples for 3 general categories: (A) events with high NO₂ TSCDs and relatively high PE, (B) events with medium PE, and (C) events with PE of almost 0. For all examples, spatial patterns are displayed, showing the NO₂ TSCD, the respective cloud fraction (FRESCO, Wang et al., 2008), and the detected WWLLN lightning strokes, where colour indicates the flash time with respect to the SCIAMACHY overpass. Table 2 lists the properties for the selected events.

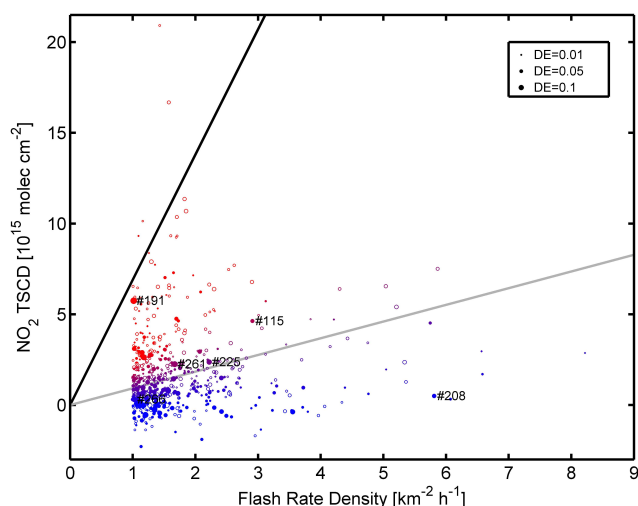


Fig. 2. NO₂ TSCDs for the events of high lightning activity with FRD > 1 /km²/h. As in Fig. 1, color codes P_{event} , and open circles indicate “polluted” events. The black line reflects the expectation (according to Eqs. 1 and 4) of 6.9×10^{15} molec/cm² per 1 /km²/h, or $P=15 \times 10^{15}$ molec/flash. The grey line represents the lower bound ($P=2 \times 10^{15}$ molec/flash) given in Schumann and Huntrieser (2007).

Category A: high NO₂ TSCDs

Figure 3 shows two examples of relatively high NO₂ TSCDs of 4.6×10^{15} molec/cm² (Event #115, south of Italy) and 5.8×10^{15} molec/cm² (Event #191, east of Florida) for the “events”, i.e. the respective ground pixels with FRD > 1/km²/h. Production Efficiencies P_{event} are 3.5×10^{25} (#115) and 12.3×10^{25} (#191) molec/flash, respectively, almost reaching the best estimate given in Schumann and Huntrieser (2007).

However, in both cases, several neighbouring pixels (even hundreds of km afar) show TSCDs of more than 6×10^{15} molec/cm² as well, whereas the lightning activity detected by WWLLN is rather localized at the event, and the spatial correlation of NO₂ TSCDs and FRD is rather poor ($R=0.04$ (#115)/ 0.25 (#191)). The large plumes of enhanced NO₂ thus indicate contributions from other NO_x sources. In Appendix C, we analyse these events in more detail and discuss how far these enhanced NO₂ TSCDs can be explained by aged LNO_x or continental outflow of anthropogenic NO_x.

Category B: medium PE

Figure 4 shows two illustrative examples for events with different lightning characteristics, where a NO₂ response to lightning could be identified. Event #261 (Malaysia) is a mesoscale convective system with more than 500 km extent. The respective NO₂ TSCDs are slightly enhanced, and the maximum TSCD of 2.3×10^{15} molec/cm² coincides with the maximum FRD of 1.7 /km²/h. Spatial pat-

terns of flashes and NO₂ TSCDs correlate quite well ($R=0.47$), supporting the interpretation of the NO₂ TSCDs to be due to lightning. However, the overall NO₂ TSCD is rather small compared to our expectation, and P_{event} is only 2.9×10^{25} molec/flash. Event #225 (Timor) is an example for a very localized lightning event, where two neighbouring pixels exceed the FRD threshold of 1 /km²/h, but no lightning occurs outside. Again, NO₂ is enhanced at the event (and only there; $R=0.52$), but TSCDs are only moderately enhanced (2.4×10^{15} molec/cm² maximum), and P_{event} is 2.3×10^{25} molec/flash. Note that such events are rather rare; only 11 events out of 287 have a spatial correlation coefficient of >0.4.

Category C: “Zero” PE

In contrast to these examples, where we can at least claim a spatial correlation of flashes and enhanced NO₂, though the enhancement is lower than expected, Fig. 5 shows events with no detectable NO₂ enhancement at all. For event #266 (north of Venezuela), NO₂ TSCDs are as few as 0.3×10^{15} molec/cm² for a FRD of 1 /km²/h; the neighbouring pixels show no indication of LNO_x outflow neither. Similarly, for event #208 (Malaysia), a very high FRD of 5.8 is observed, but NO₂ TSCDs are below 0.5×10^{15} molec/cm² for the respective ground pixel, whereas expected TSCDs according to Eqs. (4) and (1) would be as high as 40×10^{15} molec/cm², which is two orders of magnitude higher. P_{event} are 0.7×10^{25} and 0.2×10^{25} molec/flash, respectively, for both events.

4 Discussion

We performed a systematic search for satellite NO₂ observations coinciding with high lightning activity. According to literature values for PE, the high FRD over individual ground pixels would result in clearly enhanced TSCDs. But in contrast to that expectation, the observed NO₂ TSCDs are generally far lower than expected, and show no correlation with WWLLN flash counts. Our findings are even more surprising given the fact that we do not consider flashes “older” than one hour and should thus estimate an *upper* bound of LNO_x production, since our estimate of flash counts is a lower bound.

In the following, we discuss the different event categories for the examples shown in Sect. 3. We investigate how far our results might be affected by the assumptions and characteristics of

- the NO₂ retrieval (Sect. 4.1),
- the satellites’ sensitivity for lightning NO_x (Sect. 4.2),
- the WWLLN DE (Sect. 4.3),

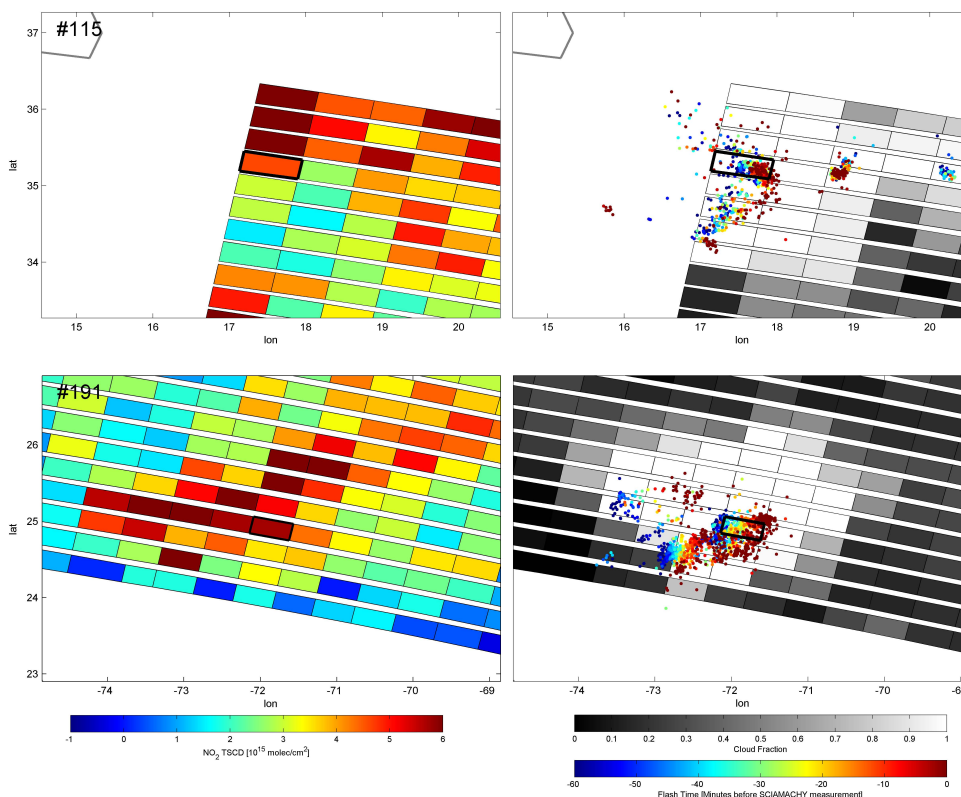


Fig. 3. Events #115 on 16 October 2006 (top) and #191 on 12 May 2007 (bottom). Left: NO₂ TSCD. Right: FRESKO Cloud fraction (greyscale) and time of individual WWLLN flashes relative to the SCIAMACHY measurement (color).

- our definition of high lightning activity (Sect. 4.4),
- or our calculation of the PE (Sect. 4.5).

Finally, we discuss possible impacts of the observed high variability of PE on estimates of LNO_x production in literature (Sect. 4.6), and evaluate possible reasons which might cause these differences in PE (Sect. 4.7).

Category A: high NO₂ TSCDs

As shown in Fig. 1, most events of (relatively) high P_{event} are observed in the Gulf of Mexico and east from Florida. This possibly indicates that PE is above average for the US, where deep convective updraft speeds are particularly high (Del Genio et al., 2007) and extreme precipitation is relatively frequent (Zipser et al., 2006). In fact, many reports of high PE in literature are based on measurements over the US, e.g. Hudman et al. (2007) ($P \approx 30 \times 10^{25}$ molec/flash), Langford et al. (2004) ($P \approx 58 \times 10^{25}$ molec/CG flash) or Ott et al. (2010) ($P \approx 22\text{--}42 \times 10^{25}$ molec/flash, including also observations over Europe). Thus, one has to keep in mind that PE is likely regional dependent, and US estimates might not be representative globally.

For many of these high-PE events, like in event #191 (see Fig. 3), the patterns of enhanced NO₂ TSCDs cannot be explained by the flashes of the last hour. Thus, aged LNO_x, or the outflow of anthropogenic NO_x, lifted up by convection, probably contributes significantly to the observed NO₂ TSCDs. The latter has to be taken into account when quantifying LNO_x in the vicinity of “polluted” regions like the US eastcoast, where Bertram et al. (2007) estimated the fraction of air originating from the planetary boundary layer in convective outflow as 0.17 ± 0.02 . I.e., convection alone can cause high NO₂ TSCDs over polluted regions. This might partly explain the cluster of generally high PE found around the US For event #191, there are indications for interference of anthropogenic NO_x and possibly also biomass burning NO_x, as shown in Appendix C. For such events where additional contributions from aged LNO_x or continental outflow of anthropogenic/biomass burning NO_x are not negligible (but hard to quantify), the estimated P_{event} are generally too high.

By our definition of events of high lightning activity and the calculation of P_{event} , we demand a spatial coincidence of lightning and NO₂ signal. It has to be noted that if we would instead consider the averaged NO₂ TSCD and the averaged FRD over a larger region of e.g. $300 \times 600 \text{ km}^2$ (i.e. 10×10 SCIAMACHY pixels), we would end up with

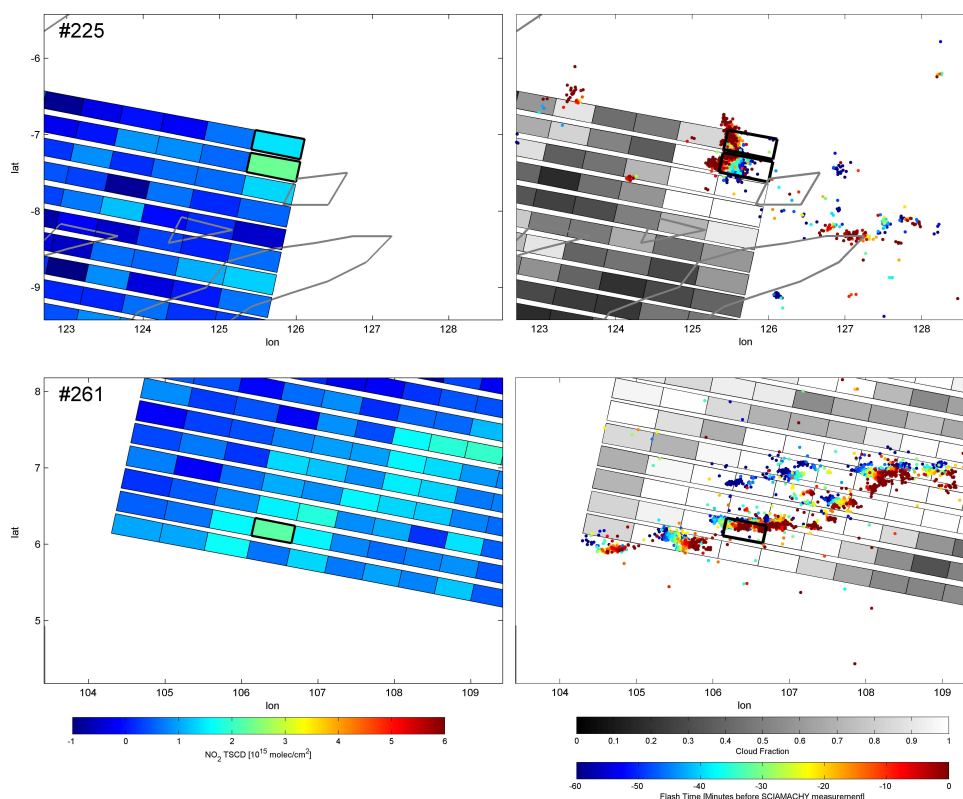


Fig. 4. Events #225 on 22 November 2007 (top) and #261 on 13 May 2008 (bottom). Left: NO₂ TSCD. Right: FRESKO Cloud fraction (greyscale) and time of individual WWLLN flashes relative to the SCIAMACHY measurement (color).

a tremendously high PE of about 300×10^{25} molec/flash for event #191. Even if we account for flashes over the last 10 flashes, PE would still be as high as 62×10^{25} molec/flash, despite the fact that large parts of the enhanced NO₂ plume show no spatial correlation with the observed flashes. This underlines the importance of identifying enhanced NO₂ TSCDs being due to lightning by demanding consistent spatial patterns of NO₂ and FRD. We therefore analyze their relationship for individual satellite ground pixels instead of calculating large-scale spatial means (see also Sect. 4.5).

Category B: medium P_{event}

In some cases, moderately enhanced NO₂ TSCDs have been found which show consistent spatial patterns with WWLLN flashes (see Fig. 4). These examples demonstrate that, in some cases, it is actually possible to detect LNO_x from space, based on a clear spatial correlation of flashes and enhanced NO₂ TSCD. The values for P_{event} of about $2\text{--}3 \times 10^{25}$ molec/flash are lower than the best estimate given in Schumann and Huntrieser (2007), but are within the range of uncertainty of $2\text{--}40 \times 10^{25}$ molec/flash. Note that a PE of 3×10^{25} molec/flash would correspond to a total annual flash production of about 1 Tg N yr^{-1} .

Category C: “Zero” P_{event}

The majority of events show no significantly enhanced NO₂ TSCDs at all, also causing an overall correlation coefficient of about 0 between FRD and NO₂ TSCD. The estimated values for P_{event} are orders of magnitude below the range reported in literature. From the quantities listed in Table 2, or the spatial patterns of flashes, we could not find an indication for what makes these “zero”-events different from the other. E.g., PE is not correlated with FRESKO cloud heights.

In the following, we discuss how far our assumptions and the characteristics of the used datasets could explain our findings, focussing particularly on those “zero” NO₂ events.

4.1 NO₂ column densities

In this study we focus on NO₂ observations over active lightning systems, i.e. over cumulonimbus clouds. Such bright clouds may potentially affect the DOAS retrieval in two ways:

- Bright clouds might lead to saturation of the detected radiances, with hardly predictable consequences for the spectral retrieval of NO₂ SCDs. We thus checked the uncalibrated detector counts (binary units) per co-adding over high clouds, and found values lower than

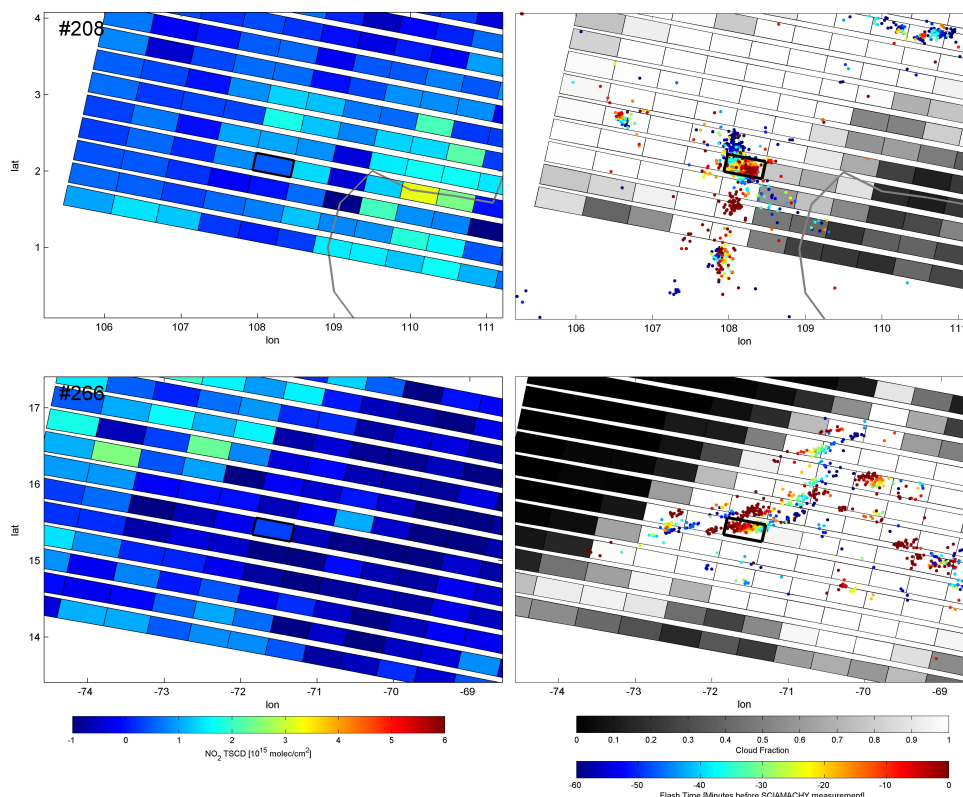


Fig. 5. Events #208 on 20 August 2007 (top) and #266 on 15 July 2008 (bottom). Left: NO₂ TSCD. Right: FRESKO Cloud fraction (greyscale) and time of individual WWLLN flashes relative to the SCIAMACHY measurement (color).

maximum counts measured at higher latitudes (with longer integration times). In addition, the fit residuals show no increased values over high clouds.

- b. Clouds affect the observed spectral structures in different ways, for instance by polarization effects (as SCIAMACHY is polarization dependent). Also inelastic scattering due to rotational and vibrational Raman is affected by clouds. Another effect of clouds is the shielding of (spectral dependent) absorbers below, including spectral reflectance at the ground. In particular over oligotrophic oceans with low chlorophyll concentrations, absorption and vibrational Raman scattering in liquid water affects the NO₂ retrieval (see also Beirle et al., 2010). Changes of the DOAS-fit settings indeed reveal slight cloud interferences: The contrast of NO₂ TSCDs for clouded versus cloud-free ground pixels over the remote Pacific depends on fit settings like polynomial degree and spectral window. However, these effects are only in the range of some 10¹⁴ molec/cm².

The derived TSCDs are – by definition of the stratospheric correction – *excess* TSCDs with respect to the Pacific. Consequently,

- a. negative (unphysical) TSCD occasionally occur in case of a local overestimation of the stratospheric column, and
- b. we generally underestimate real *clear-sky* NO₂ TSCDs by about 0.5×10^{15} molec/cm² (Martin et al., 2002). However, we can not simply add such an offset to the NO₂ TSCDs used in this study, since the NO₂ TSCDs of interest are observed under *cloudy* conditions, affecting the NO₂ AMFs. It is difficult to quantify this effect, as, in addition, convection also modifies the *profile* of the background NO₂; the uplift of NO₂ generally leads to increased AMFs, i.e. higher TSCDs. But this is partly compensated by a concurrent decrease of the NO₂/NO_x ratio (see also Beirle et al., 2009). However, the Pacific tropospheric background is quite small (compared to the expected response in NO₂ TSCD due to LNO_x) and thus does not affect our general findings.

4.2 Sensitivity of satellite observations for freshly produced LNO_x

For the translation of NO₂ TSCDs to NO_x TVCDs, we apply the sensitivity E of 0.46, as derived by Beirle et al. (2009) from a one-week episode of a thunderstorm simulation by a cloud resolving chemistry model. The model run covers all

stages of thunderstorm evolution and thus allows to estimate E for a large variety of atmospheric conditions, while the simulated sensitivities for individual model columns show a surprisingly low variability. In particular, E is almost independent on cloud optical thickness, i.e. the sensitivities for core, anvil, and outflow regimes are quite similar. Above all, almost no pixels with zero sensitivity have been found, i.e. the model does not reproduce situations in which the LNO_x is completely hidden from the satellite's view. The derived sensitivities are also robust with respect to vertical shifts of the NO_x profile (see Beirle et al., 2009).

Model results generally are subject to uncertainties, and the simulated (maritime) thunderstorm might not be representative for all thunderstorms investigated in this current study. However, the general pattern of the profiles of NO₂ box-AMFs (high at the cloud top and decreasing towards the cloud bottom) and of the NO₂/NO_x ratio (low at the cloud top and increasing towards the cloud bottom) are basic properties of (cumulonimbus) clouds, which automatically results in a maximum sensitivity at the cloud middle. As soon as LNO_x is present there, it becomes visible from space. Thus, the only plausible explanation for a scenario of completely "hidden" LNO_x would be a situation with all LNO_x placed below the cloud. Such LNO_x profiles might result from CG flashes occurring downwind (instead of inside) the updraft cores (compare Dye et al., 2000). However, such exclusively below-cloud LNO_x profiles are contrary to the commonly accepted "C-shape". In contrast, for LNO_x profiles with a large fraction of NO_x in the middle troposphere, as have been recently simulated by Ott et al. (2010), the sensitivity of satellite measurements for LNO_x would be even higher than 0.46.

4.3 WWLLN

The annual DE of WWLLN was estimated by a quite simple comparison of annual FRD to the LIS/OTD climatology (see Appendix A1). As the addition of stations to WWLLN can happen on any day within the year, the estimated annual mean DE maps are systematically too high for some regions up to the date when a new station is added, and too low afterwards. In addition, lightning statistics may not be sufficient after just one year, especially over oceanic regions, where also statistics of the LIS/OTD climatology are poor. Both effects are definitely causing rather high error bars in the estimated DE, and thus would dampen the expected correlation of FRD to NO₂ TSCDs. However, these errors are to a large part of statistical nature, and thus can not explain the discrepancy of the absolute level of NO₂ TSCDs to our expectation. In addition, a particular focus on events for high DE of about 10% and more (in 2007 and 2008), where estimated FRD are more reliable, results in basically the same findings.

We also investigated the diurnal cycle of the WWLLN DE by comparison with the LIS/OTD diurnal cycle (see Appendix A2). We found no indication that DE is signifi-

cantly different for the SCIAMACHY observation time of 10:00 a.m. local time.

To further check the estimated DE of WWLLN D_{clim} , we also directly compared the number of individual flash counts from WWLLN to LIS flash counts whenever a coincident TRMM overpass occurred (Appendix A3). We therefore define "coincidence" as a LIS measurement containing the SCIAMACHY pixel center within a time window of 2 h before up to 1 h after the SCIAMACHY time. As LIS is an orbiting satellite, the observation duration at a specific location is rather short (about 1 min). Nevertheless, we found 42 out of 287 events, where coincident LIS measurements are available. For these coincidences, we compared LIS flash counts to WWLLN flash counts in the same time interval within the LIS field of view, thereby estimating also an *instantaneous* DE D_{inst} . The resulting values D_{inst} are presented and discussed in Appendix A3.

The comparison of D_{clim} and D_{inst} (Fig. A6c in Appendix A3) reveals a large scatter, which is expected due to the short time period of coincident observations. In addition, D_{inst} , derived from coincident LIS measurements, is systematically higher (by a factor of about 3) than D_{clim} derived from the LIS/OTD climatology. This is an interesting finding, which can not be explained by the diurnal cycle of the WWLLN DE (see Appendix A2). Instead, it indicates a systematically higher DE for the selected events of high flash rate densities. This higher DE is likely related to above-average peak currents: Abarca et al. (2010) report on a distinct morning-time maximum of WWLLN flashes with high peak currents (see Fig. 5d therein). The WWLLN DE for such high peak-current flashes would be above average (the relation of DE and peak currents is almost linear up to 50 kA, Rodger et al., 2009), and our demand for high FRD probably selects events with high peak-current flashes.

If we use D_{inst} instead of D_{clim} for the calculation of PE, the results are on average higher by a factor of 2.8 (for the 42 coincidences). One could thus argue that we generally have to scale our resulting PE by a factor of 3 accordingly. But as long as the increased instantaneous DE is due to above-average peak currents, we would also expect that the respective flashes have LNO_x production P above average, since high current flashes also produce more LNO_x. This is also an almost linear effect, as shown in Wang et al. (1998). Thus, the observed discrepancy between FRD and NO₂ TSCD remains more or less the same, as both effects (the increase in DE, thus the decrease in FRD, and the increase in PE due to high-current flashes) cancel each other out largely.

4.4 Definition of events of "high" lightning activity

One has to keep in mind that SCIAMACHY measurements are performed at about 10:00 a.m. LT. Thus, the selection of events of high lightning activity coinciding with SCIAMACHY is rather special, and the respective flashes may not be representative. In particular, most events have been found

over ocean, where lightning activity is quite independent from daytime, while continental flashes show a strong afternoon peak (in addition, some continental events are skipped due to probable interference of anthropogenic NO_x).

Our indications for rather low LNO_x production may thus be specific for maritime morning-time flashes. However, we performed a similar case study using OMI observations (02:00 p.m.) which generally yields the same results (though the spatial correlation of TSCDs to FRD is more complex due to the smaller OMI ground pixel sizes).

4.5 Relation of NO₂ TSCDs and WWLLN FRD

For our estimation of the LNO_x production per flash, we assume that the produced LNO_x stays within the SCIAMACHY pixel for the considered time window of one hour. We thus neglect (a) chemical loss, which is well justified as the lifetime of NO₂ is of the order of days in the upper troposphere, and (b) dilution and outflow.

We argue that this neglect is admissible, as the dimension of SCIAMACHY ground pixels is about 30 × 60 km². The movement of the flash cluster, which can be tracked by the color-coded flash time in Figs. 3–5, indicates wind speeds of the same order of magnitude, i.e. 30–60 km/h.

We are aware that still some fraction of the LNO_x is “lost” by outflow from the SCIAMACHY ground pixel. However, this is at least partly compensated by some inflow of LNO_x from neighbouring pixels, which is neglected as well in our study. In addition, also the FRD is generally underestimated due to the restriction to 1 h.

The event maps generally do not indicate a considerable enhancement of the neighbouring TSCDs in wind direction (as indicated by the movement of WWLLN flashes). Thus, we see no evidence that outflow to neighbouring pixels would let us seriously overlook the produced LNO_x by focussing on the single event groundpixel. In particular, outflow can not explain the findings of virtual no NO₂, like e.g. for event #266.

From a sensitivity study, involving also the NO₂ TSCDs of the 8 direct neighbouring ground pixels, we conservatively estimate the loss of LNO_x due to transport being less than 50%, i.e. the PEs might be underestimated up to 100%. But even if the estimated PEs would be doubled, the discrepancy to literature values remains.

4.6 High variability of PE

We observe a very high variability of NO₂ TSCDs and PE for the detected lightning events. This is, to some extent, in accordance to a very wide range of reported NO_x levels in and around thunderstorms and estimates of PE in literature (Schumann and Huntrieser, 2007). This wide range might be partly related to difficulties in aircraft observations, different lightning detection systems, and fundamental shortcomings in measurement techniques, and thus may just reflect

the high observational uncertainties. But we might have to accept that lightning itself is a highly variable phenomenon, and PE is a highly variable quantity, varying strongly from thunderstorm to thunderstorm, and even from flash to flash. Consequently, one has to be aware that published estimates of PE are potentially biased towards too high values, since any finding of significantly enhanced NO_x in the vicinity of lightning is likely to be published, while measurements of no or low levels of NO_x might be discarded. This phenomenon is known as “publication bias” (e.g., Scargle et al., 2000).

Our category B results are in accordance to a LNO_x production of the order of 2–3 × 10²⁵ molec/flash, which is at the lower end of current estimates (Schumann and Huntrieser, 2007). However, the low PE values for category C results are far below any value reported in literature.

4.7 Factors determining PE

Several quantities have been discussed in literature to be determinative for the PE, i.e. the LNO_x produced per flash.

As a consequence of the Zel’dovich mechanism, PE increases with energy and peak current (Wang et al., 1998). Flashes of low peak current are thus less productive concerning LNO_x. This might in principle be a possible explanation for lightning without NO₂ production (category C). However, as we use FRDs based on WWLLN flash counts, we implicitly (at least partly) account for this: a thunderstorm with flashes of low peak current would probably produce only a small amount of NO_x, but due to dependency of WWLLN DE on peak current, only few flashes would be detected. The threshold of $F > 1$ /km²/h thus selects, at the same time, events with many flashes as well as events with not too low peak currents. Since both, WWLLN DE and PE, increase almost linearly with peak current, we probably can not explain the category C events by less productive flashes due to low peak currents.

Huntrieser et al. (2008) report on relatively low PE for tropical thunderstorms during the TROCCINOX campaign in Brazil, in contrast to subtropical thunderstorms, and could relate this to a difference in average stroke lengths. They propose that tropical thunderstorms have generally shorter flash lengths, and are thus generally less productive with respect to LNO_x/flash, than subtropical thunderstorms, as a consequence of enhanced vertical wind shear of the latter. In Huntrieser et al. (2009) correlations of P with vertical wind shear are reported using in-situ measurements from the TROCCINOX and SCOUT-O₃ campaigns.

Indeed, Fig. 1 reveals a latitudinal dependency of P_{event} , showing higher values in the subtropics. However, this is mainly a consequence of the high values for P_{event} close to the US Eastcoast and in the Mediterranean, as represented by the category A examples #115 and #191. As discussed before, for these events, high NO₂ TSCDs are observed also for pixels without recent lightning activity, indicating the impact of aged LNO_x and/or outflow of anthropogenic pollution, so

that the observed latitudinal dependency of P_{event} should not be overinterpreted. But at least most events with low P are indeed tropical events, which might thus be less productive due to low wind shears.

Huntrieser et al. (2009) also proposed that warm rain processes, which might be dominant for the tropical morning-time thunderstorms of this study, may result in very short flash components. I.e., though the detected events show – by selection – high FRD, these flashes might generally be less productive in producing NO_x compared to flashes for mixed-phase precipitation processes with probably longer flash channels. To check whether the detected events show mixed-phases, we investigated Polarization-Corrected Temperatures (PCTs) from the 37 and 85 GHz Radar TMI onboard TRMM, whenever coinciding (see Appendix B). For several events, quite low PCTs are observed (<210 K down to <180 K at 37 GHz, and <110 K down to <70 K at 85 GHz), which classify the respective events as intense thunderstorms (Zipser et al., 2006) and indicate the presence of hail (Cecil, 2009). The PCT at 37 GHz is slightly anticorrelated to P_{event} ($R = -0.51$, see Fig. B1 in Appendix B), i.e. PE tends to be higher for low PCT, which might indeed indicate a link of mixed-phase precipitation and lightning PE, but statistics of this comparison are rather poor, and there are still some events with low PCT (<201 K) and yet low PE.

Obviously, lightning is a very complex phenomenon, resulting in high variability of PE, and systematic dependencies on several parameters which are still poorly understood. Aiming for one single value of P (or, as a first specification, two universal values P_{IC} and P_{CG}) is probably not appropriate for the representation of global LNO_x production. The simple relation of P to flash properties like energy, peak current, or flash length is a first step, but increases the observational needs.

Further diversification of flash characteristics is probably needed. Rahman et al. (2007) measured the LNO_x production from rocket-triggered lightning and conclude that steady currents, and not return strokes, are the primary LNO_x producers. Cooray et al. (2009) analyzed the produced number of NO_x molecules for various flash processes in the laboratory, and confirm that return strokes produce relatively few NO_x, while other processes such as leaders or continuing currents are rather important.

Thus, one hypothesis which could explain the absence of LNO_x for events of high lightning activity might be the occurrence of flashes with strong return strokes, making the flashes “visible” for LIS and WWLLN, but low steady currents (producing small amounts of LNO_x). However, this is quite speculative and hard to substantiate with the currently available lightning datasets on global scale.

5 Conclusions

We performed a systematic investigation of SCIAMACHY measurements of NO₂ for coincident lightning events with high flash rate densities as observed by WWLLN, resulting in 287 “events”. For each event, an individual estimate for the Production Efficiency (PE, i.e. LNO_x production per flash) is derived.

In contrast to our a-priori expectation of clearly enhanced NO₂ column densities due to the considered high flash rate densities, the resulting values for PE are highly variable, and far below literature values. Surprisingly, NO₂ column densities do not correlate with flash rate densities.

For some events, strongly enhanced NO₂ column densities are observed. But the spatial pattern of NO₂ cannot be explained by the fresh flashes alone; instead, aged LNO_x and/or continental outflow of anthropogenic pollution contributes significantly.

Few events show a good spatial correlation of flashes and enhanced NO₂ column densities. For these events, PE was rather low ($2\text{--}3 \times 10^{25}$ molec/cm²), which would correspond – by simple extrapolation – to a global annual LNO_x production of the order of 1 Tg N.

The majority of the events has very low PE ($<1 \times 10^{25}$ molec/flash). We do not see any reason to abandon these events as artefacts or outliers. However, we could not find any characteristics of these less productive events making them different from the others (except that they are mostly, but not exclusively, at low latitudes), and find no plausible explanation for these events. Further investigations have to reveal how far these low estimates of PE are related to the implicit and explicit selections of events due to the WWLLN detection efficiency, SCIAMACHY observation time, the pollution mask, and the focus on high flash rate densities, resulting in active morning-time thunderstorms, mostly over oceans. From the continental events of this study, however, we come to essentially the same conclusions.

Overall, our results are not consistent with the current estimates of P of about $15(2\text{--}40) \times 10^{25}$ molec/flash. While this might be related to the specifics of morning time flashes and our focus on high FRD, it could also indicate that PE is overestimated in literature. We see two possible reasons for this:

1. PE estimates in literature might be generally biased high (“publication bias”, Scargle et al., 2000): Observations of high PE (“positive” results) have likely been published, while observations of low PE (“negative” results) might have been discarded as non-significant or non-conclusive. But for the estimation of a sound, unbiased mean, information on both tails of the statistical distribution of the NO_x production per flash is needed. We encourage feedback to this hypothesis from scientists having performed in-situ measurements.

2. A large fraction of estimates of NO_x production by lightning is based on experiments performed in the US, for several reasons: there is a large scientific community, a good infrastructure (lightning networks, aircraft campaigns), and lightning activity is generally high as well. From our study, we find highest PE around the US. This might be related to higher flash lengths of subtropical thunderstorms, but could also simply be a consequence of uplifted anthropogenic pollution. In either case, extrapolations of PE estimates over the US to global scale are possibly too high.

Obviously, the matter of NO_x production by lightning still leaves many questions open, and lightning characteristics are probably too complex to be reasonably represented by just one universal number for PE. Within the ongoing studies on LNO_x production, the analysis of satellite measurements of NO₂ allows an independent approach, complementing laboratory and in-situ measurements.

Appendix A

The detection efficiency of WWLLN

A1 DE from LIS/OTD climatology

For a quantitative relation of NO₂ TSCDs to FRD, the number of flashes actually measured by WWLLN has to be scaled according to the respective detection efficiency (DE). Thus, estimates of WWLLN DE are required as function of time and place. For this purpose, we calculate mean annual FRD from individual WWLLN flash counts on a map of 1° resolution for each year 2004–2008 (Fig. A2), and set them in relation to the FRD from LIS/OTD climatology (Fig. A1) (see LIS/OTD documentation, 2007) to define the climatological DE D_{clim} (Fig. A3) according to Eq. (2).

To avoid biased DE caused by strong localized thunderstorms (which may potentially lead to high local FRD above average and thus to a too low DE estimate), both, LIS/OTD and WWLLN FRD are spatially smoothed by a Gaussian function with $\sigma = 1.5^\circ$. Note that flash rate densities are generally low over oceans, and the climatological FRDs are derived from the extrapolation of rather few actual flash counts (typically 10–30 for a FRD of 1 flashes/km²/year). We thus skip regions with $F_{\text{LIS/OTD}} < 1$ flashes/km²/year, to avoid division by small numbers with respective high uncertainties. For the remaining oceanic regions, statistical fluctuations are still significant, but partly eliminated by the applied spatial smoothing.

Figure A3 shows the resulting DE for 2005 and 2008 exemplarily. DE is highest over Australia and Indonesia, as WWLLN evolved from a regional network initiated in New Zealand (Dowden et al., 2008). Over the years, the number of participating stations increased from 19 (2004) to 30 (2007) (Rodger et al., 2009), which improves the DE also for

other parts of the world, in particular for central and northern America.

The DE of 2005 can be compared to the estimate given in Rodger et al., 2006 (Figs. 13 and 14 therein), for April 2005, showing generally similar spatial patterns. However, a quantitative comparison also shows large deviations. Differences are expected for mainly two reasons: First, Rodger et al. (2006) estimate DE for one day (16 April 2005), while Fig. A3 shows our mean annual DE. Second, Rodger et al. (2006) explicitly estimate the DE for CG flashes (though WWLLN also detects IC flashes with sufficient peak currents), while our climatological approach based on LIS/OTD results in an “effective” DE for total (IC+CG) flashes. Consequently, we expect our DE to be lower by a factor of about 4 (for a IC/CG ratio of 3). One striking difference is that our estimated DE shows a clear land-ocean contrast, which is not visible in the estimate by Rodger et al. (2006). This is probably related to a land-ocean contrast in the DE of WWLLN, which is expected, since VLF radio waves propagate with less attenuation over seawater than over land. However, Lay et al. (2007) found only a small effect, with DE over ocean being 13% higher (relative) than over land. The observed land-sea contrast might also be related to LIS/OTD characteristics, or a change in the IC/CG ratio between continents and oceans.

Jacobson et al. (2005) investigate WWLLN DE for both IC and CG flashes over Florida in summer 2004 by comparisons to the Los Alamos Sferic Array, and estimate a mean DE of about 1% for the considered region around 29° N, 82° W. This is in good agreement with our estimated DE for this location in 2004 (0.9%).

A further study on WWLLN DE has been published recently by Abarca et al. (2010), using the US national lightning detection network (NLDN) as ground truth. In Table 2 therein, they number the WWLLN DE (for CG+IC flashes) over the US for 2007–2008 as 2.9%, matching pretty well our value for this period and region (1.8% in 2007 and 3.9% in 2008).

A2 Diurnal cycle of WWLLN DE

The climatological WWLLN DE defined above accounts for total flash counts independent of time of day, while our consideration of coincident SCIAMACHY measurements selects events at about 10:00 a.m. local time. We thus also investigate the diurnal cycle of the WWLLN DE by comparing WWLLN flash counts, grouped in 1-h bins according to local time, to the climatological LIS/OTD diurnal cycle, which is available on a 2.5° grid. We investigate the diurnal cycle of WWLLN DE separately for continents and oceans by (a) gridding the WWLLN flash counts to the same grid as the LIS/OTD climatology, (b) integrating the flash counts of the respective continental/oceanic grid pixels for both WWLLN and LIS/OTD, and (c) defining DE for each hourly bin as ratio of the respective WWLLN and LIS/OTD flash counts.

Coastal grid pixels, containing both ocean and continent, are skipped.

The diurnal cycles of LIS/OTD and WWLLN flash counts show the known afternoon peak over continents, and a minimum at about 10:00 a.m. (Fig. A4a, b). The time-shift of the afternoon peak of WWLLN relative to LIS/OTD might be related to the fact that different regions show different local times of the peak (Lay et al., 2007), and the regions are contributing differently to the total number of flashes for LIS/OTD than for WWLLN due to the regionally varying DE. Over oceans, the diurnal variations are small and show no clear pattern.

Over continents, mean WWLLN DE (Fig. A4c) is 1.9% at night and 1.5% at day. The slightly higher nighttime DE is in accordance with Abreu et al. (2010) and is likely related to the effect of day/night ionospheric changes on VLF wave propagation. However, the DE over oceans (8.2% for both day and night) does not show a clear day/night pattern, but instead only moderate fluctuations (of the order of $\pm 10\%$ relative change), which may partly be caused by statistical fluctuations due to the low number of flash counts for both LIS/OTD and WWLLN over oceans (compare Fig. A4b).

A3 DE from concurrent LIS overpasses

In addition to the comparison of WWLLN FRD to the LIS/OTD climatology, we also compared the flashes detected by WWLLN and LIS for individual lightning events. Of course, this approach requires coincident LIS overpass. If we search for LIS overpasses containing the event location within a time window of 2 h before up to 1 h after the event, and demand at least 5 LIS flashes during overpass, we find 42 of such coincidences. LIS flash counts and WWLLN flash counts within the LIS overpass time are shown in Fig. A5 for two events. In addition, also TRMM PCTs are displayed (see Appendix B).

The selected events illustrate two opposing situations: For event #64, LIS counts 68 flashes, while WWLLN detects 2 flashes, which corresponds to our expectation according to the respective climatological DE of 2.3%. Event #171, on the other hand, is an example for a case where WWLLN flash counts (19) are almost as high as LIS flash counts (23), despite a climatological DE of 8.4%. LIS measurements have taken place 99 min before/43 min after the SCIAMACHY measurement, respectively.

For a quantitative comparison, we sum up LIS flash counts as well as the respective WWLLN flash counts within the LIS field of view for each coincidence. Figure A6a displays the respective flash counts. In Fig. A6b, corrected flash counts are shown: WWLLN flash counts are scaled by $1/D_{\text{clim}}$, while LIS flash counts are scaled by $1/0.7$, according to the DE of LIS of 70% at 10:00 a.m. Figure A6c displays the “instantaneous” WWLLN DE D_{inst} , defined as ratio of (actual) WWLLN and (corrected) LIS flash counts:

$$D_{\text{inst}} := N_{\text{WWLLN}}/N_{\text{LIS}}^{\text{corr}}, \quad (\text{A1})$$

The ratio of two flash counts for a region of about $640 \times 640 \text{ km}^2$ (LIS field of view) and a time interval of the order of 1 min (LIS overpass time at the event) is of course rather uncertain, and statistical deviations to the climatological DE are not surprising. Nevertheless, Fig. A6b and c indicate that instantaneous DE are *systematically* higher (on average by a factor of about 3) than the climatological ones.

The observed systematically enhanced instantaneous DE can not be explained by the diurnal cycle of WWLLN DE. Instead, it is probably a consequence of our focus on events with high FRD: Abarca et al. (2010) report on a distinct morning-time peak of WWLLN flashes with high peak currents (see Fig. 5c therein). Such high peak currents would be well detectable by WWLLN, which is strongly dependent on peak currents (approx. linear for a wide range of peak currents see Rodger et al., 2009).

Appendix B

Polarization corrected temperatures from TRMM

There are indications that PE might be related to warm rain vs. mixed-phase precipitation processes (Huntrieser et al., 2009). Thus, in order to investigate the presence of hail for the detected lightning events, we also analyzed polarization-corrected temperatures (PCT) from brightness temperature measurements of TMI on TRMM for the coincident overpasses as defined in Appendix A. PCT are calculated as defined in Spencer et al. (1989) (for 85 GHz, see Eq. 3 therein) and Cecil et al. (2002) (for 37 GHz, see Eq. 2 therein). Low PCT are indicators for intense thunderstorms and the presence of hail (Toracinta and Zipser, 2001; Zipser et al., 2006; Cecil, 2009). PCT at 37 GHz is shown as background greyscale map in Fig. A5 (Appendix B). As expected, the flash locations generally coincide with low PCT. For each available event, we define a “minimum PCT” by the minimum PCT value within a range of 200 km from the respective event. Figure B1 shows the correlation of minimum PCT at 37 GHz with (a) minimum PCT at 85 GHz, (b) LIS flash counts, and (c) NO₂ TSCD. PCTs at 37 GHz and 85 GHz are strongly correlated. Minimum PCT at 37/85 GHz reach values down to $<180/ <70 \text{ K}$, respectively, which are extremely low values (compare Zipser et al., 2006) and are strongly indicating hail (Cecil, 2009). Generally, events with low PCT at 37 GHz also show low PCT at 85 GHz, but for some events PCT at 85 GHz is low (about 100 K), but medium for 37 GHz (about 220 K). LIS flash counts tend to be higher for low PCT, but the scatter is quite high due to the short time interval of LIS overpass. Also the NO_x PE per flash shows a slight tendency to be higher for low PCT, which would correspond to the hypothesis of higher LNO_x PE for flashes from intense thunderstorms. However, the scatter is high ($R = -0.54$), and there are still several cases with low PCT (about 200 K) and low PE.

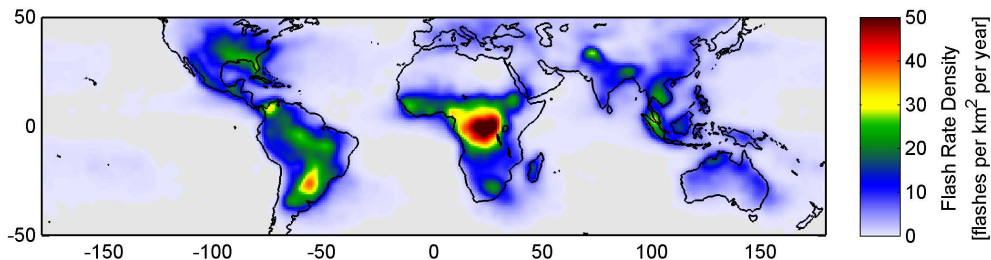


Fig. A1. Global map of the LIS/OTD climatological flash rate densities.

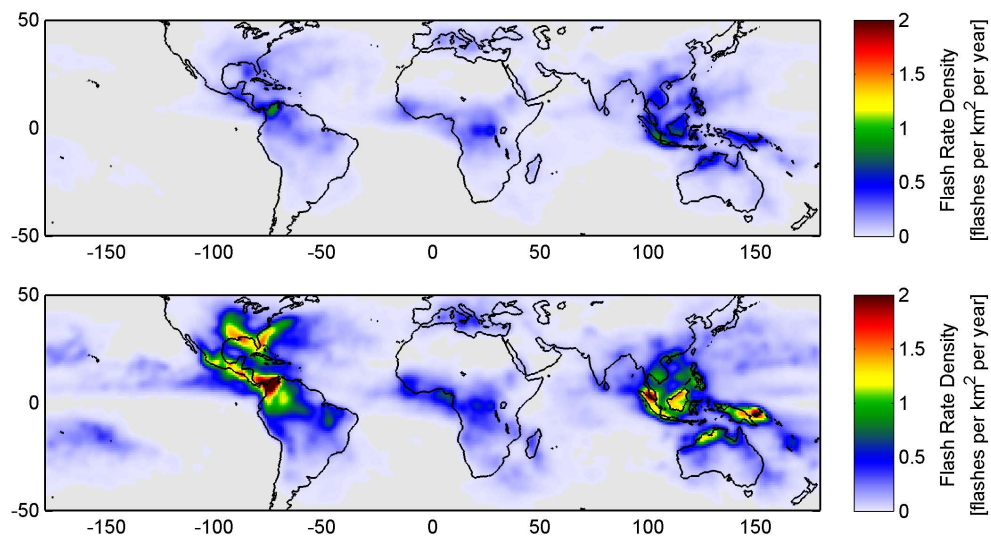


Fig. A2. Global map of the WWLLN flash rate density (uncorrected) in 2005 (top) and 2008 (bottom).

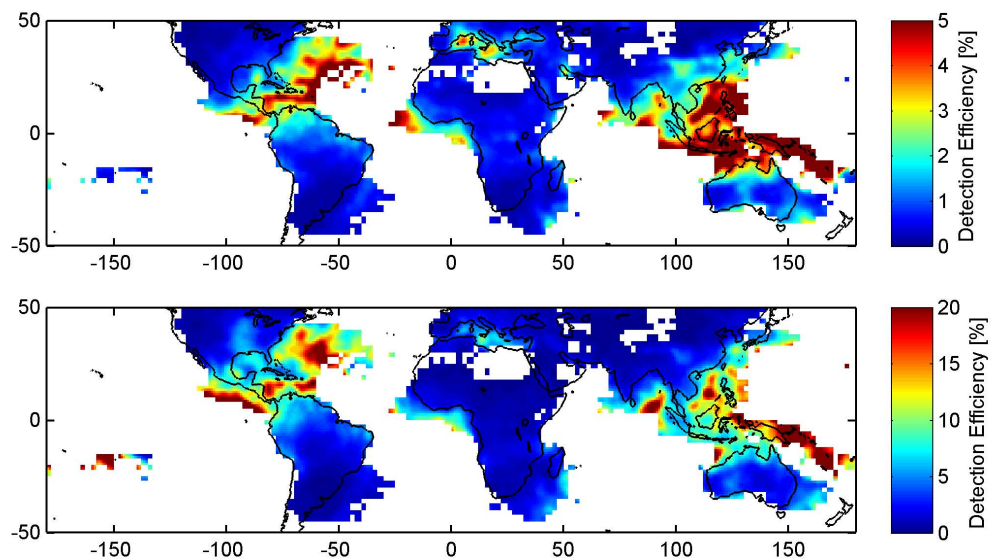


Fig. A3. Global map of the WWLLN detection efficiency D_{clim} for 2005 (top) and 2008 (bottom). Note that the colorscales are different.

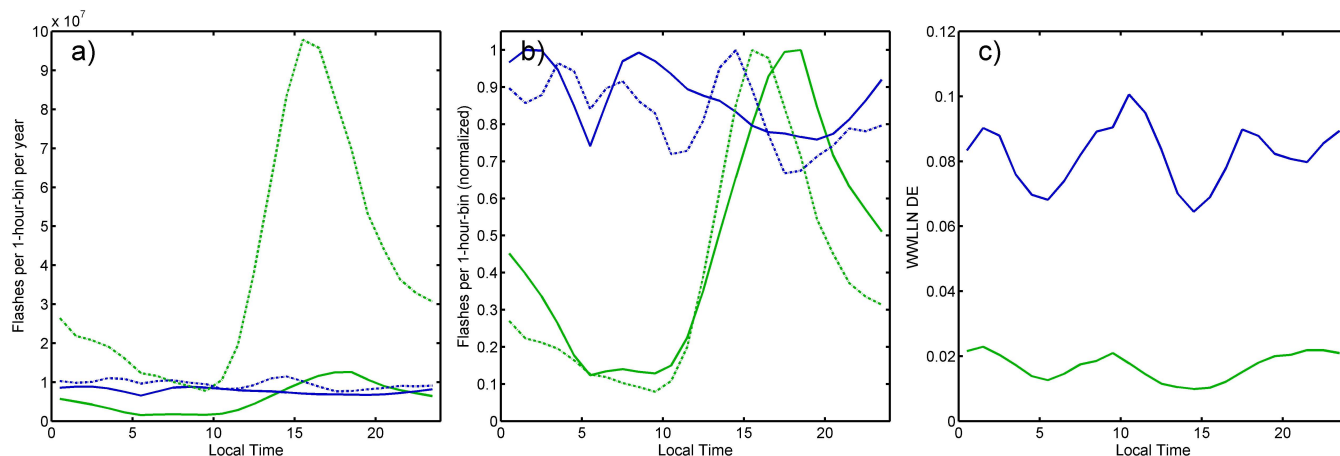


Fig. A4. Diurnal cycle of LIS/OTD (dotted) and WWLLN (straight) flash counts and WWLLN DE over oceans (blue) and continents (green). **(a)** Total number of flashes per 1-h bin and per year. WWLLN flash counts have been scaled up by a factor of 10. **(b)** Normalized diurnal patterns of flash counts per 1-h bin. **(c)** Diurnal cycle of the WWLLN DE, defined as the ratio of the diurnal patterns of total flash counts as shown in (a).

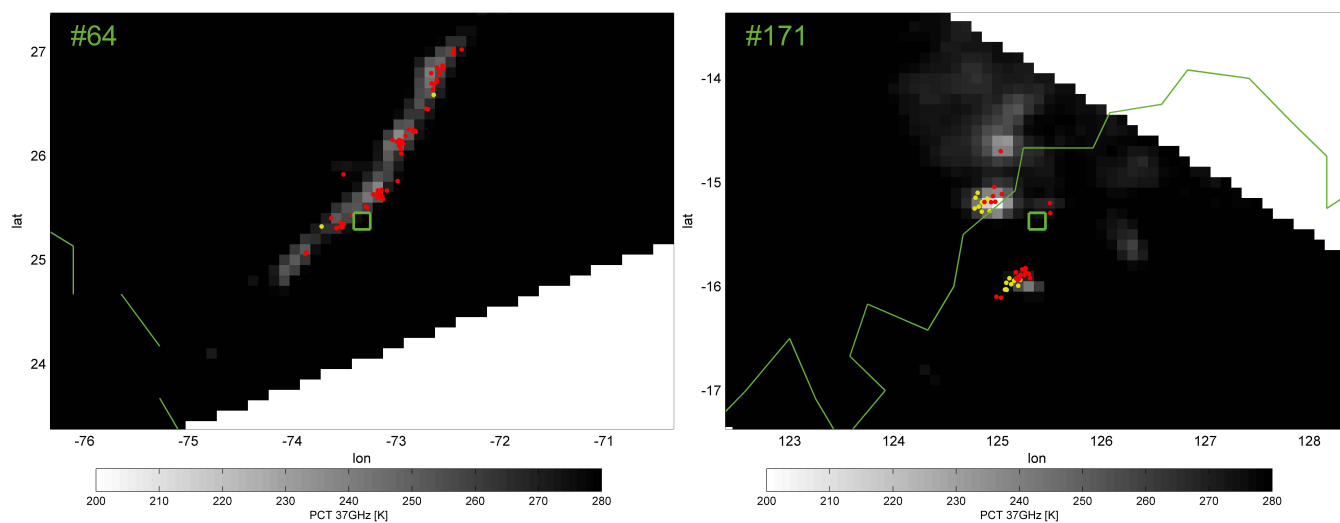


Fig. A5. TRMM overpasses close to the SCIAMACHY measurements for event #64 (top) and #171 (bottom). Red dots are flashes detected by LIS (68/23), while yellow dots are WWLLN flashes detected within the LIS overpass time (2/19). The green square marks the center coordinates of the respective SCIAMACHY pixels. The respective climatological DEs are 2.3% and 8.4%, while the instantaneous DEs are 2.1% and 57.8%, respectively. Greyscale background shows the PCT at 37 GHz (minimum: 233 K (#64)/202 K (#171)) (see Appendix B).

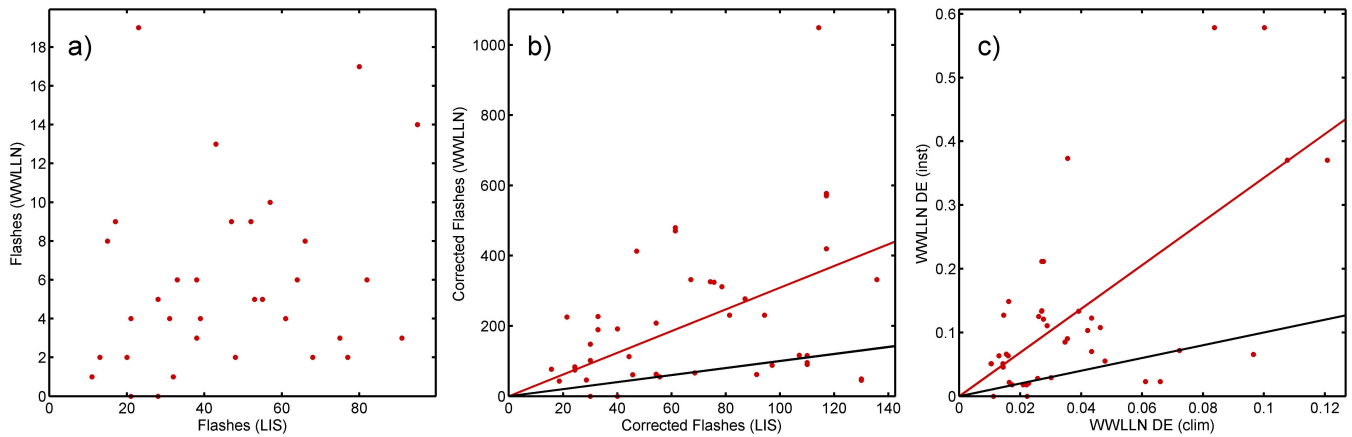


Fig. A6. Comparison of flash counts from LIS and WWLLN for LIS overpasses coinciding with SCIAMACHY for events of high lightning activity. (a) Scatterplot of the number of original flash counts from LIS and WWLLN. (b) Correlation ($R = 0.35$) of corrected flash counts from LIS (scaled by $1/0.7$) and WWLLN (scaled by $1/D_{\text{clim}}$). The black line corresponds to 1:1. The slope of the fitted line through origin (red) is 3.1. (c) Correlation ($R = 0.63$) of D_{clim} (Eq. 2) and D_{inst} (Eq. A1). The black line corresponds to 1:1. The slope of the fitted line through origin (red) is 3.4.

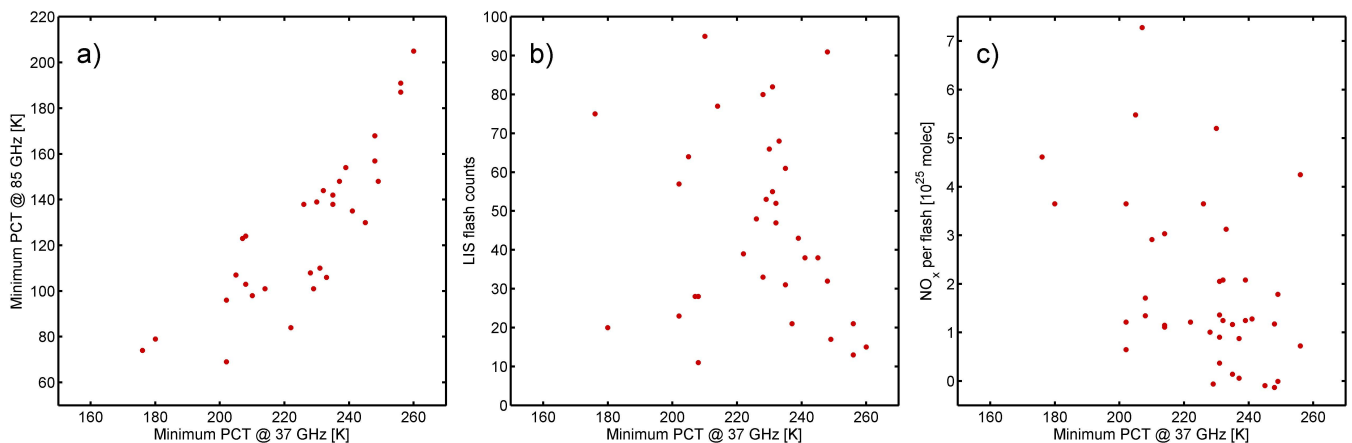


Fig. B1. Correlation of minimum PCT at 37 GHz with (a) minimum PCT at 85 GHz ($R = 0.84$), (b) number of LIS flash counts ($R = -0.14$), and (c) the production efficiency P_{event} ($R = -0.51$), for the coincident TRMM overpasses.

Appendix C

High NO_2 events

In the discussions of category A events (high NO_2 TSCD), we argue that the pattern of enhanced NO_2 for events #115 and #191 can not be explained by fresh LNO_x production alone, but is probably due to aged LNO_x and/or continental outflow of anthropogenic pollution. To support this hypothesis, we additionally analyzed (a) the flashes of the previous 40 h, (b) HYSPLIT backtrajectories, and (c) MOPITT CO and SCIAMACHY absorbing aerosol index (AAI) observations.

- Figure C1 shows the occurrence of WWLLN flashes back to 40 h prior to the SCIAMACHY measurement for events #115 and #191. Note that the clipping displays a larger region compared to Fig. 3. Again, dots indicate the time of WWLLN flashes relative to the SCIAMACHY measurement, but now up to 40 h back. The SCIAMACHY ground pixel of the respective event is shown as black rectangle.

High lightning activity several hours back in time can be observed for both events.

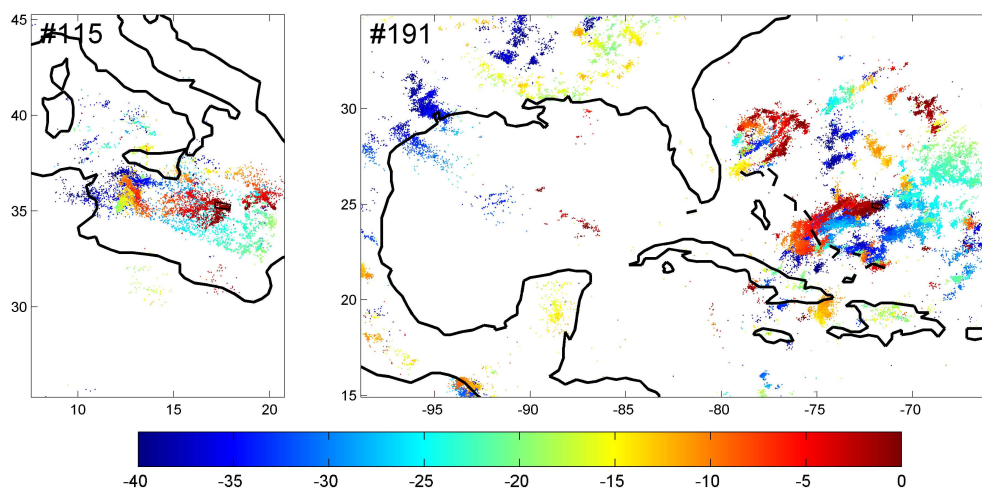


Fig. C1. Occurrence of WWLLN flashes back to 40h prior to the SCIAMACHY measurement for events #115 (left) and #191 (right). Note that the clipping shows a larger region compared to Fig. 3. Dots indicate the time of WWLLN flashes relative to the SCIAMACHY measurement up to 40h back. The respective SCIAMACHY ground pixels of the events of high lightning activity are shown as black rectangles.

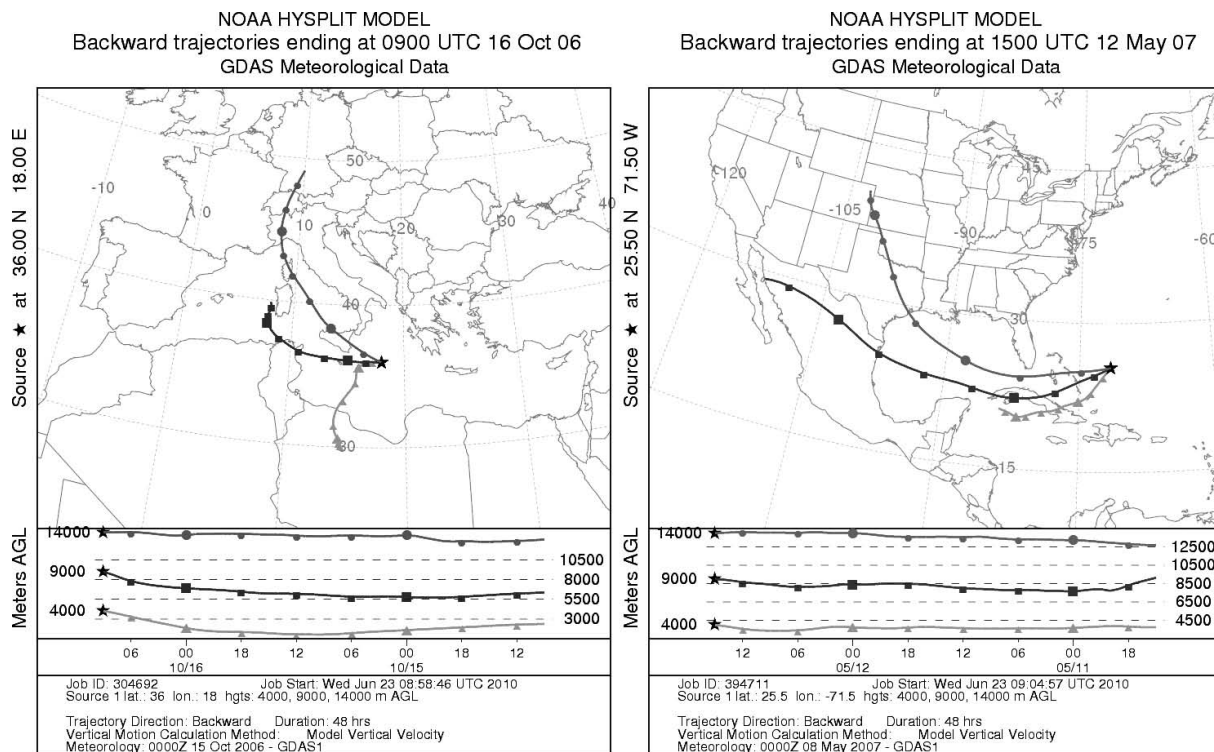


Fig. C2. HYSPLIT backtrajectories from the event location over 48 h for 3 different altitudes for events #115 (left) and #191 (right). Air-masses of continental (polluted) origin can only be identified for transport in the upper troposphere.

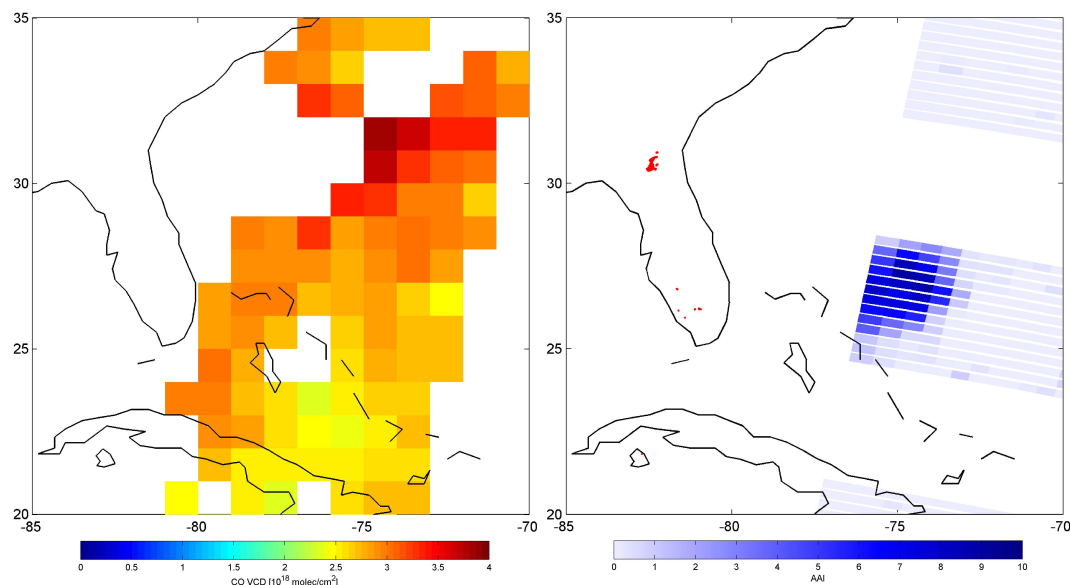


Fig. C3. Left: MOPITT CO VCD on 12 May 2007. Right: SCIAMACHY absorbing aerosol index (AAI) (Penning de Vries et al., 2009) on 12 May 2007. The red dots indicate fires detected by ATSR on 11 May 2007.

- b. Figure C2 shows HYSPLIT backtrajectories, starting at the event, over 48 h for three different altitudes in the middle and upper troposphere.

For event #115, the backtrajectory at 9 km altitude crosses the region south of Sicily where high lightning activity was observed over the last 40 h. The backtrajectory at 14 km altitude indicates transport from continental Europe; the Po-valley in northern Italy is generally highly polluted with respect to NO₂. However, from the WWLLN flash counts, we found no indication of deep convection over this region which would be necessary to uplift the boundary layer pollution to the upper troposphere.

For event #191, again the backtrajectories match the track of WWLLN flashes over the last hours. In addition, the backtrajectory at 14 km altitude indicates transport from continental US; in this case, we actually find indication of deep convection about 40 h ago over Houston, Texas (Fig. C1b), which might have uplifted anthropogenic NO_x to the upper troposphere, from where it might have been transported to the event location.

- c. Figure C3 shows MOPITT CO VCD and the SCIAMACHY AAI. Both datasets show enhanced values in the vicinity of event #191, but the spatial patterns do not match perfectly. The enhanced CO VCDs might again indicate anthropogenic outflow, but the high AAI clearly indicates biomass burning. In fact, ATSR detected fires in Florida on 11 May 2007, as also shown in Fig. C3.

Thus, though the different datasets do not reveal a clear and simple explanation for the expanded plume of enhanced NO₂ TSCD on 12 May 2007, there are strong indications that other sources than lightning have contributed significantly.

Acknowledgements. Steffen Beirle was funded by the DFG (Deutsche Forschungsgemeinschaft, German research society). We thank ESA and DLR for providing SCIAMACHY spectra. The authors wish to thank the World Wide Lightning Location Network (<http://wwlln.net>), a collaboration among over 40 universities and institutions, for providing the lightning location data used in this paper. The v1.0 gridded satellite lightning data were produced by the NASA LIS/OTD Science Team (Principal Investigator, Hugh J. Christian, NASA/Marshall Space Flight Center) and are available from the Global Hydrology Resource Center (<http://ghrc.msfc.nasa.gov>). NASA is acknowledged for providing TRMM (<http://mirador.gsfc.nasa.gov/>) and LIS (<http://thunder.nsstc.nasa.gov/data/>) data. We thank the TEMIS team for providing SCIAMACHY cloud fractions (FRESCO+, <http://www.temis.nl>). We acknowledge NOAA Air Resources Laboratory for providing the HYSPLIT trajectory model (<http://ready.arl.noaa.gov/HYSPLIT.php>). MOPITT CO measurements are provided by NASA. SCIAMACHY Aerosol Absorbing Index data was provided by Marloes Penning de Vries. ATSR fire counts were taken from the World Fire Atlas from the Data User Element of the European Space Agency. We thank Craig Rodger, Bob Holzworth and Ken Pickering for helpful discussions, and two anonymous reviewers for their constructive comments during the open discussion process.

The service charges for this open access publication have been covered by the Max Planck Society.

Edited by: B. N. Duncan

References

- Abarca, S. F., Corbosiero, K. L., and Galarneau, T. J.: An evaluation of the Worldwide Lightning Location Network (WWLLN) using the National Lightning Detection Network (NLDN) as ground truth, *J. Geophys. Res.*, 115(D18), D18206, doi:10.1029/2009JD013411, 2010.
- Arnone, E., Kero, A., Dinelli, B. M., Enell, C. F., Arnold, N. F., Papandrea, E., Rodger, C. J., Carlotti, M., Ridolfi, M., and Turunen, E.: Seeking sprite-induced signatures in remotely sensed middle atmosphere NO₂, *Geophys. Res. Lett.*, 35, L05807, doi:10.1029/2007GL031791, 2008.
- Beirle, S., Platt, U., Wenig, M., and Wagner, T.: NO_x production by lightning estimated with GOME, *Adv. Space Res.*, 34(4), 793–797, 2004.
- Beirle, S., Spichtinger, N., Stohl, A., Cummins, K. L., Turner, T., Boccippio, D., Cooper, O. R., Wenig, M., Grzegorski, M., Platt, U., and Wagner, T.: Estimating the NO_x produced by lightning from GOME and NLDN data: a case study in the Gulf of Mexico, *Atmos. Chem. Phys.*, 6, 1075–1089, doi:10.5194/acp-6-1075-2006, 2006.
- Beirle, S., Salzmann, M., Lawrence, M. G., and Wagner, T.: Sensitivity of satellite observations for freshly produced lightning NO_x, *Atmos. Chem. Phys.*, 9, 1077–1094, doi:10.5194/acp-9-1077-2009, 2009.
- Beirle, S., Kühl, S., Pukite, J., and Wagner, T.: Retrieval of tropospheric column densities of NO₂ from combined SCIAMACHY nadir/limb measurements, *Atmos. Meas. Tech.*, 3, 283–299, doi:10.5194/amt-3-283-2010, 2010.
- Bertram, T., Perring, A., Wooldridge, P., Crounse, J., Kwan, A., Wennberg, P., Scheuer, E., Dibb, J., Avery, M., Sachse, G., Vay, S., Crawford, J. H., McNaughton, C. S., Clarke, A., Pickering, K. E., Fuelberg, H., Huey, G., Blake, D. R., Singh, H. B., Hall, S. R., Shetter, R. E., Fried, A., Heikes, B. G., and Cohen, R. C.: Direct measurements of the convective recycling of the upper troposphere, *Science*, 315(5813), 816–820, doi:10.1126/science.1134548, 2007.
- Boersma, K. F., Eskes, H. J., and Brinksma, E. J.: Error analysis for tropospheric NO₂ retrieval from space, *J. Geophys. Res.*, 109, D04311, doi:10.1029/2003JD003962, 2004.
- Boersma, K. F., Eskes, H. J., Meijer, E. W., and Kelder, H. M.: Estimates of lightning NO_x production from GOME satellite observations, *Atmos. Chem. Phys.*, 5, 2311–2331, doi:10.5194/acp-5-2311-2005, 2005.
- Bovensmann, H., Burrows, J. P., Buchwitz, M., Frerick, J., Noël, S., Rozanov, V. V., Chance, K. V., and Goede, A. P. H.: SCIAMACHY: Mission objectives and measurement modes, *J. Atmos. Sci.*, 56(2), 127–150, 1999.
- Bucsela, E. J., Pickering, K. E., Huntemann, T. L., Cohen, R. C., Perring, A., Gleason, J. F., Blakeslee, R. J., Albrecht, R. I., Holzworth, R., Cipriani, J. P., Vargas-Navarro, D., Mora-Segura, I., Pacheco-Hernández, A., and Laporte-Molina, S.: Lightning-generated NO_x seen by OMI during NASA's TC4 experiment, *J. Geophys. Res.*, 115, D00J10, doi:10.1029/2009JD013118, 2010.
- Cecil, D. J., Zipser, E. J., and Nesbitt, S. W.: Reflectivity, Ice Scattering, and Lightning Characteristics of Hurricane Eyewalls and Rainbands. Part I: Quantitative Description, *Mon. Weather Rev.*, 130(4), 769–784, 2002.
- Cecil, D. J.: Passive microwave brightness temperatures as proxies for hailstorms, *J. Appl. Meteorol. Clim.*, 48(6), 1281–1286, 2009.
- Christian, H. J., Blakeslee, R. J., Boccippio, D. J., Boeck, W. L., Buechler, D. E., Driscoll, K. T., Goodman, S. J., Hall, J. M., Koshak, W. J., Mach, D. M., and Stewart, M. F.: Global frequency and distribution of lightning as observed from space by the Optical Transient Detector, *J. Geophys. Res.*, 108, 4005, doi:10.1029/2002JD002347, 2003.
- Cooray, V., Rahman, M., and Rakov, V.: On the NO_x production by laboratory electrical discharges and lightning, *J. Atmos. Sol.-Terr. Phys.*, 71(17–18), 1877–1889, 2009.
- Del Genio, A. D., Yao, M.-S., and Jonas, J.: Will moist convection be stronger in a warmer climate?, *Geophys. Res. Lett.*, 34, L16703, doi:10.1029/2007GL030525, 2007.
- Dowden, R. L., Brundell, J. B., and Rodger, C. J.: VLF lightning location by time of group arrival (TOGA) at multiple sites, *J. Atmos. Sol.-Terr. Phys.*, 64, 817–830, 2002.
- Dowden, R. L., Holzworth, R. H., Rodger, C. J., Lichtenberger, J., Thomson, N. R., Jacobson, A. R., Lay, E., Blundell, J. B., Lyons, T. J., O'Keefe, S., Kawasaki, Z., Price, C., Prior, V., Ortega, P., Weinman, J., Mikhailov, Y., Veliz, O., Qie, X., Burns, G., Collier, A., Diaz, R., Adamo, C., Williams, E. R., Kumar, S., Raga, G. B., Rosado, J. M., Avila, E. E., Cliverd, M. A., Ulich, T., Gorham, P., Shanahan, T., Osipowicz, T., Cook, G., and Zhao, Y.: World-wide lightning location using VLF propagation in the Earth-Ionosphere waveguide, *IEEE Antenn. Propag. M.*, 50(5), 40–60, 2008.
- Dye, J. E., Ridley, B. A., Skamarock, W., Barth, M., Venticinque, M., Defer, E., Blanchet, P., Thery, C., Laroche, P., Baumann, K., Hubler, G., Parrish, D. D., Ryerson, T., Trainer, M., Frost, G., Holloway, J. S., Matejka, T., Bartels, D., Fehsenfeld, F. C., Tuck, A., Rutledge, S. A., Lang, T., Stith, J., and Zerr, R.: An overview of the stratospheric-tropospheric experiment: radiation, aerosols and ozone (STERAO)-deep convection experiment with result from the July 10, 1996 storm, *J. Geophys. Res.*, 105, 10023–10045, 2000.
- Hild, L., Richter, A., Rozanov, V., and Burrows, J. P.: Air mass calculations for GOME measurements of lightning-produced NO₂, *Adv. Space Res.*, 29(11), 1685–1690, 2002.
- Hudman, R. C., Jacob, D. J., Turquety, S., Leibensperger, E. M., Murray, L. T., Wu, S., Gilliland, A. B., Avery, M., Bertram, T. H., Brune, W., Cohen, R. C., Dibb, J. E., Flocke, F. M., Fried, A., Holloway, J., Neuman, J. A., Orville, R., Perring, A., Ren, X., Sachse, G. W., Singh, H. B., Swanson, A., and Wooldridge, P. J.: Surface and lightning sources of nitrogen oxides over the United States: Magnitudes, chemical evolution, and outflow, *J. Geophys. Res.*, 112, D12S05, doi:10.1029/2006JD007912, 2007.
- Huntrieser, H., Schumann, U., Schlager, H., Höller, H., Giez, A., Betz, H.-D., Brunner, D., Forster, C., Pinto Jr., O., and Calheiros, R.: Lightning activity in Brazilian thunderstorms during TROCINOX: implications for NO_x production, *Atmos. Chem. Phys.*, 8, 921–953, doi:10.5194/acp-8-921-2008, 2008.
- Huntrieser, H., Schlager, H., Lichtenstern, M., Roiger, A., Stock, P., Minikin, A., Höller, H., Schmidt, K., Betz, H.-D., Allen, G., Viciani, S., Ulanovsky, A., Ravegnani, F., and Brunner, D.: NO_x production by lightning in Hector: first airborne measurements during SCOUT-O3/ACTIVE, *Atmos. Chem. Phys.*, 9, 8377–8412, doi:10.5194/acp-9-8377-2009, 2009.
- Jacobson, A., Holzworth, R., Harlin, J., Dowden, R., and Lay, E.:

- Performance assessment of the World Wide Lightning Location Network (WWLLN), using the Los Alamos Sferic Array (LASA) as ground truth, *J. Atmos. Ocean. Technol.*, 23(8), 1082–1092, 2006.
- Labrador, L. J., von Kuhlmann, R., and Lawrence, M. G.: The effects of lightning-produced NO_x and its vertical distribution on atmospheric chemistry: sensitivity simulations with MATCH-MPIC, *Atmos. Chem. Phys.*, 5, 1815–1834, doi:10.5194/acp-5-1815-2005, 2005.
- Langford, A. O., Portmann, R. W., Daniel, J. S., Miller, H. L., and Solomon, S.: Spectroscopic measurements of NO₂ in a Colorado thunderstorm: Determination of the mean production by cloud-to-ground lightning flashes, *J. Geophys. Res.*, 109, D11304, doi:10.1029/2003JD004158, 2004.
- Lay, E. H., Holzworth, R. H., Rodger, C. J., Thomas, J. N., Pinto Jr., O., and Dowden, R. L.: WWLL global lightning detection system: Regional validation study in Brazil, *Geophys. Res. Lett.*, 31(3), L03102, doi:10.1029/2003GL018882, 2004.
- Lay, E. H., Jacobson, A. R., Holzworth, R. H., Rodger, C. J., and Dowden, R. L.: Local time variation in land/ocean lightning flash density as measured by the World Wide Lightning Location Network, *J. Geophys. Res.*, 112, D13111, doi:10.1029/2006JD007944, 2007.
- LIS/OTD documentation: LIS/OTD Gridded Products V 2.2: 1995–2005, Documentation and Examples, 1 September 2006, http://ghrc.nsstc.nasa.gov/uso/ds_docs/lis_climatology/lis_otd_gridded_products_documentation_v2.2.pdf, last access: March 2010, 2007.
- Martin, R. V., Chance, K., Jacob, D. J., Kurosu, T. P., Spurr, R. J. D., Bucsela, E., Gleason, J. F., Palmer, P. I., Bey, I., Fiore, A. M., Li, Q., Yantosca, R. M., and Koелеmeijer, R. B. A.: An improved retrieval of tropospheric nitrogen dioxide from GOME, *J. Geophys. Res.*, 107(D20), 4437, doi:10.1029/2001JD001027, 2002.
- Martin, R. V., Sauvage, B., Folkins, I., Sioris, C. E., Boone, C., Bernath, P., and Ziemke, J.: Space-based constraints on the production of nitric oxide by lightning, *J. Geophys. Res.*, 112, D09309, doi:10.1029/2006JD007831, 2007.
- Martin, R. V.: Satellite remote sensing of surface air quality, *Atmos. Environ.*, 42, 7823–7843, 2008.
- Ott, L. E., Pickering, K. E., Stenchikov, G. L., Allen, D. J., DeCaria, A. J., Ridley, B., Lin, R.-F., Lang, S., and Tao, W.-K.: Production of lightning NO_x and its vertical distribution calculated from three-dimensional cloud-scale chemical transport model simulations, *J. Geophys. Res.*, 115, D04301, doi:10.1029/2009JD011880, 2010.
- Penning de Vries, M. J. M., Beirle, S., and Wagner, T.: UV Aerosol Indices from SCIAMACHY: introducing the SCattering Index (SCI), *Atmos. Chem. Phys.*, 9, 9555–9567, doi:10.5194/acp-9-9555-2009, 2009.
- Price, C. and Rind, D.: What determines the cloud-to-ground lightning fraction in thunderstorms?, *Geophys. Res. Lett.*, 20, 463–466, 1993.
- Rahman, M., Cooray, V., Rakov, V. A., Uman, M. A., Liyanage, P., DeCarlo, B. A., Jerauld, J., and Olsen, R. C.: Measurements of NO_x produced by rocket-triggered lightning, *Geophys. Res. Lett.*, 34, L03816, doi:10.1029/2006GL027956, 2007.
- Rodger, C. J., Brundell, J. B., Dowden, R. L., and Thomson, N. R.: Location accuracy of long distance VLF lightning location network, *Ann. Geophys.*, 22, 747–758, doi:10.5194/angeo-22-747-2004, 2004.
- Rodger, C. J., Werner, S., Brundell, J. B., Lay, E. H., Thomson, N. R., Holzworth, R. H., and Dowden, R. L.: Detection efficiency of the VLF World-Wide Lightning Location Network (WWLLN): initial case study, *Ann. Geophys.*, 24, 3197–3214, doi:10.5194/angeo-24-3197-2006, 2006.
- Rodger, C. J., Brundell, J. B., Holzworth, R. H., and Lay, E. H.: Growing Detection Efficiency of the World Wide Lightning Location Network, *Am. Inst. Phys. Conf. Proc.*, Coupling of thunderstorms and lightning discharges to near-Earth space: Proceedings of the Workshop, Corte (France), 23–27 June 2008, 1118, 15–20, doi:10.1063/1.3137706, 2009.
- Scargle, J. D.: Publication bias: the file-drawer problem in scientific inference, *J. Sci. Explor.*, 14(2), 94–106, 2000.
- Schumann, U. and Huntrieser, H.: The global lightning-induced nitrogen oxides source, *Atmos. Chem. Phys.*, 7, 3823–3907, doi:10.5194/acp-7-3823-2007, 2007.
- Spencer, R. W., Goodman, H. M., and Hood, R. E.: Precipitation retrieval over land and ocean with the SSM/I: Identification and characteristics of the scattering signal, *J. Atmos. Ocean. Tech.*, 6, 254–273, 1989.
- Wagner, T., Beirle, S., Deutschmann, T., Eigemeier, E., Frankenberg, C., Grzegorski, M., Liu, C., Marbach, T., Platt, U., and Penning de Vries, M.: Monitoring of atmospheric trace gases, clouds, aerosols and surface properties from UV/vis/NIR satellite instruments, *J. Opt. A, Pure Appl. Opt.*, 10, 104019, doi:10.1088/1464-4258/10/10/104019, 2008.
- Wang, Y., DeSilva, A. W., Goldenbaum, G. C., and Dickerson, R. R.: Nitric oxide production by simulated lightning: Dependence on current, energy, and pressure, *J. Geophys. Res.*, 103, 19149–19159, 1998.
- Wang, P., Stammes, P., van der A, R., Pinardi, G., and van Roozendael, M.: FRESCO+: an improved O₂ A-band cloud retrieval algorithm for tropospheric trace gas retrievals, *Atmos. Chem. Phys.*, 8, 6565–6576, doi:10.5194/acp-8-6565-2008, 2008.
- Zipser, E. J., Cecil, D. J., Liu, C., Nesbitt, S. W., and Yorty, D. P.: Where are the most intense thunderstorms on Earth?, *B. Amer. Meteorol. Soc.*, 87, 1057–1071, 2006.